

## REVIEW

# Vibration-based bridge scour detection: A review

Ting Bao<sup>1</sup> | Zhen Liu<sup>2\*</sup>

<sup>1</sup>Department of Civil and Environmental Engineering, Michigan Technological University, 1400 Townsend Drive, Dow 854, Houghton, Michigan 49931, USA

<sup>2</sup>Department of Civil and Environmental Engineering, Michigan Technological University, 1400 Townsend Drive, Dillman 201F, Houghton, Michigan 49931, USA

**Correspondence**

Zhen (Leo) Liu, Department of Civil and Environmental Engineering, Michigan Technological University, 1400 Townsend Drive, Dillman 201F, Houghton, Michigan 49931, USA.  
Email: zhenl@mtu.edu

**Summary**

Scour around bridge foundations are regarded as one of the predominant causes of bridge failures. Traditional methods primarily employ underwater instruments to detect bridge scour depths, which thus have difficulties in instrument installations and operations. The concept of scour detection derived from vibration-based damage detection has been explored in recent years to address such difficulties by investigating the natural frequency spectrum of a bridge or a bridge component. This paper presents a comprehensive review of existing studies on scour detection using the natural frequency spectrum of a bridge or a bridge component. Underlying mechanisms, laboratory and field tests, numerical studies, and data processing schemes are reviewed to summarize the state of the art, which is absent but urgently needed. Updates on recently developed scour monitoring sensors are also provided to complement the introduction. Based on the review, in-depth discussions in existing studies are made regarding a few controversial and unsolved issues to shed light on future research, highlighting issues such as the soil–structure interaction, locations of the sensor installation, and the influence of shapes of scour holes.

**KEYWORDS**

bridge scour detection, data processing scheme, natural frequency, sensor monitoring, soil–structure interaction

## 1 | INTRODUCTION

Scour around bridge foundations is regarded as one of the predominant factors in inducing bridge failures.<sup>[1–3]</sup> Elsaid<sup>[4]</sup> reported that more than 603,168 bridges existed in the United States and 12% of these bridges have structural deficiencies. Among them, 58% within 1,500 bridges collapsed in the past 40 years due to bridge scour damage,<sup>[5]</sup> resulting in a huge financial cost for bridge repairing and retrofiting. According to statistics,<sup>[6,7]</sup> the average annual cost for repairs of highways due to flood damage was 50 million; while the annual cost for scour-related bridge failures was estimated to be 30 million. Also, scour-induced bridge failures interrupt transportation and thus lead to a greater financial loss. Besides, scour-induced bridge collapses usually occur suddenly with-

people were killed. The main reason was due to the rapid development of scour holes caused by quickly washing away sediments around bridge foundations during a constant torrential rain. Therefore, this type of catastrophic failure greatly endangers human lives.

The most straightforward way to mitigate the threat of bridge scour is to estimate the scour situation using empirical or stochastic approaches. Scour is induced as flowing water excavates and removes materials around the bridge foundation from bed and bank of streams.<sup>[10]</sup> Scour assessments remain difficult because this process is coupled with many factors,<sup>[11]</sup> for example, flow, deck, pier, abutment, and soil. Factors contributing to scour formation include the geometry of the channel, dynamic hydraulic properties of the flow, and foundation configurations.<sup>[11]</sup> In the past decades, various empirical equations based on laboratory tests and field observations have been proposed to predict the scour depth in terms of different factors in constructions, scour models, parameters, laboratory or site conditions.<sup>[12–14]</sup> However, many uncertainties are involved when determining the



**FIGURE 1** Scour-induced bridge collapses. (a) Shi-Ting-Jiang Bridge failed on August 19, 2010<sup>[8]</sup>; (b) Pan-Jiang Bridge failed on March 9, 2013.<sup>[9]</sup> Both bridges were in Sichuan province, China

parameters in these equations in the field. To avoid the uncertainties, artificial neural networks were then developed to predict the scour depth.<sup>[15–18]</sup> The advantage of this method is that physical relationships between bridge scour and various factors affecting bridge scour do not need to be well defined. Due to the small errors and correlation coefficients, the predictions obtained with artificial neural networks are more satisfactory than those with empirical equations.

Numerical simulations, laboratory modeling, and in situ monitoring have also been used in evaluating the severity caused by bridge scour.<sup>[19–30]</sup> Numerical models have been applied to simulate the complicated process involving the soil–fluid–structure interaction, while laboratory models have been studied to understand the development of scour in reality under the influence of water flow and the soil–structure interaction (SSI). Results from both numerical simulations and laboratory models can be taken to better understand the relationship between different factors and scour progression. Details of mathematical modelling of scour around hydraulic and marine structures can be referred to Mutlu Sumer.<sup>[31]</sup> Up-to-date studies on flow-altering countermeasures against bridge scour including their limitations and difficulties in field applications can be found in Tafarojnoruz et al.<sup>[32]</sup> For *in situ* scour measurements, various instruments have been used for long-term monitoring. Such instruments include float-out devices, sonar apparatuses, tethered buried switches, ground penetrating radars, buried and driven rods, sound wave devices, electrical conductivity devices, and Fiber-Bragg grating sensors.<sup>[33–42]</sup> Details about the operational principles of these instruments can be found in Prendergast and Gavin<sup>[36]</sup>, and Deng and Cai.<sup>[40]</sup>

Many attempts at scour monitoring for actual bridges have also been made. Efforts, taking those in Taiwan, for example, are significant because several bridges collapsed due to scour severity, such as the Shuang-Yuan Bridge<sup>[43]</sup> and the Hou-Feng Bridge.<sup>[44]</sup> To alleviate the bridge scour threat, Lu et al.<sup>[45]</sup> conducted field experiments at the Si-Lo Bridge in the lower Cho-Shui River to detect the general scour and the total scour using a sliding magnetic collar, a steel rod, and a numbered-brick column. Lin et al.<sup>[44]</sup> used mobile location-based services for real-time monitoring of progressive scour at the Da-Jia River Bridge of National

Freeway No. 1 and No. 3. Wang et al.<sup>[46]</sup> utilized an easily installed piezoelectric film-type sensor on the piers of the Si-Bin Bridge for scour monitoring in real time. The test results from these field studies confirmed that these techniques were able to monitor the scour development of actual bridges in real time for the purpose of preventing bridges from scour-induced failures.

While the previous investigations in bridge scour detection primarily focus on scour detection with underwater instruments, a novel way derived from vibration-based damage detection has been gaining increasing attention in recent years. Difficulties such as the installation and operation of instruments in traditional methods for scour detection can be easily addressed using this innovative way by investigating the natural frequency spectrum of a bridge or a bridge component. Various studies have been presented based on the hypothesis that scour has an effect on the natural frequency spectrum of a bridge or a bridge component. However, despite the significant advances in this innovative technique, no review study has been conducted to summarize the relevant knowledge and experience learnt from the existing studies and to introduce the latest progress. To address the need, this paper presents a comprehensive review of the existing studies on bridge scour detection based on the natural frequency spectrum of a bridge or a bridge component. The existing studies are reviewed according to the following categories: laboratory and field tests, numerical studies, and data processing schemes. To complement the framework, background knowledge such as basic mechanisms is introduced firstly and updates on recent developments in scour monitoring sensors are provided afterward. In-depth discussions in the existing studies are made regarding a few controversial and unsolved issues to shed light on the future development of the technique.

## 2 | NATURAL FREQUENCY-BASED MECHANISMS AND EXCITATION METHODS

Mechanisms of how scour affects the natural frequency spectrum of a bridge or a bridge component are introduced in this section to lay down a basis for the following introduction to

the existing studies on bridge scour detection using the natural frequency spectrum. The straightforward way to obtain the natural frequency spectrum is to analyze the dynamic responses of a test component using the Fast Fourier Transform (FFT). As the natural frequency is intended to detect bridge scour, one critical issue is to understand how the scour development affects the natural frequency spectrum. Mechanisms of the frequency-based scour detection thus are firstly introduced in the 2.1. The other critical issue is to generate effective vibrations for analyzing the dynamic responses. Two general ways for generating vibrations, that is, forced vibration and ambient vibration, are introduced in the 2.2 Section. Advantages and limitations of both are summarized afterwards for the following introduction.

## 2.1 | Mechanisms of frequency spectrum-based scour detection

The presence of bridge scour leads to changes in the natural frequency spectrum of a bridge/bridge component. For general structural damage, the stiffness of the structure, which reflects in the natural frequency spectrum, is a main indicator of structural health monitoring.<sup>[47]</sup> A measured predominant natural frequency (PNF), which is substantially lower than the expected frequency, indicates an abnormal loss in the stiffness of a measured component.<sup>[1,47]</sup> Similarly, for bridge scour, taking a bridge pier for example, the stiffness of a pier is very likely to be decreased if the measured PNF of the pier is lower than the expected. The result can be clearly inferred from Equation (1)<sup>[48]</sup>:

$$f_n = \frac{1}{2\pi} \sqrt{\frac{k}{m}} \quad (1)$$

where  $f_n$  (Hz) is the PNF;  $k$  (N/m) and  $m$  (kg) are the stiffness and mass, respectively;  $\pi$  is the circumference ratio.

Two aspects, that is, mass and stiffness, have an impact on the change in the PNF. The PNF decreases if the mass of the bridge pier increases. Also, any decrease in the stiffness of the bridge pier leads to a reduction in its PNF. The pier is surrounded by soils when it is in a condition without scour. During bridge scour progression, the free length of the pier gradually increases because the top layer of the surrounding soils is eroded away by flows. In the meanwhile, the mass of the pier remains the same when the soils around the pier are removed. Accordingly, the removed soils around the pier change the boundary conditions of the pier, or to be more specific, loosen the soil constraint to the pier. The structural integrality in the pier itself remains unchanged at that situation. Therefore, an unchanged mass with a decreased stiffness results in a reduction in the PNF of the pier. In other words, the removed soils around the pier weaken the soil–pier interaction so that the lateral stiffness of the pier tends to be reduced.<sup>[49]</sup> If a scour hole develops, the lateral stiffness of the pier is further reduced. As a result, the PNF of the pier

will decrease with the bridge scour development. Because the natural frequency of the pier depends on its stiffness, observing changes in the PNF is a potential approach for scour damage identification and bridge health monitoring.<sup>[36]</sup> However, it is worthwhile to mention that structure-induced damage in reality can also lead to the change in the PNF of a bridge or a pier. This fact causes a difficulty in the framework of detecting bridge scour using the PNF if structure-induced damage happens. However, because the inspection of the bridge superstructure is usually easier, it is assumed that structure-induced damage is not considered (or known), and consequently, the change in the PNF is used to indicate changes in the scour depth.

## 2.2 | Excitation methods

### 2.2.1 | Forced vibration

Forced vibration is induced by intentional dynamic loads. Artificial vibration sources include iron balls, vibrators, hammers, and so forth. Due to the reason of artificial operations, the input force level and frequency are usually predetermined. The ratio of high desired frequency to undesired frequency (DF/UF) can be achieved prior to tests.<sup>[50]</sup> This advantage is taken to easily identify dynamic characteristics of a structure.<sup>[4]</sup> Another advantage is that the force level and frequency are not measured for signals processing, which eliminates a considerable number of extraneous noises. Due to the advantages, forced vibration such as those using rubber hammers have been successfully used for obtaining the dynamic responses of a bridge/bridge component. For instance, Biswas et al.<sup>[51]</sup> studied the indication of structural damage using forced vibration on a full-scale bridge. Shinoda et al.<sup>[52]</sup> used an iron ball to vibrate a bridge pier for estimating bridge performance after bed degradation. Yao et al.<sup>[53]</sup> utilized a hammer impact to identify dynamic responses of bridge piers in the laboratory test. An impulse hammer was used to excite free vibration on a simulated single bridge pier (a steel square hollow beam) to identify its dynamic characteristics.<sup>[54]</sup> To conclude, forced vibration is a useful way to produce desired data from which system parameters can be better identified. However, it is worthwhile to mention that forced vibration may not be suitable for old bridges as no setups are pre-made for the equipment installation.

### 2.2.2 | Ambient vibration

Ambient vibration is usually caused by unintentional man-made or atmospheric disturbances, for example, winds, floods, and passing vehicles. Different from forced vibration, ambient vibration contains many uncontrolled load functions. A low DF/UF ratio, for example, the vehicle frequency (undesired), presents in signals because ambient vibration contains high undesired noises from the exciter.<sup>[49]</sup> Also, the input is unknown, which makes it difficult to estimate dynamic signals. By contrast, the advantage of this type of vibration is that it involves convenient measurements in

real-time monitoring without causing any traffic interruption. Also, little effort is needed in the measurements. Furthermore, the ambient vibration method can provide a safer measurement environment because no operator is required to excite a measured component. Due to the advantages, much attention has been paid to ambient vibration for identifying the dynamic properties of a structure. For example, Yang and Lin<sup>[55,56]</sup> proposed to scan the PNF of a bridge using a passing vehicle. The response recorded using an accelerometer installed in the vehicle was processed with the FFT algorithm to extract the PNF of the bridge. Further studies were carried out to enhance the visibility of the first primary frequency of the bridge and to find an effective way for extracting bridge frequencies using a passing vehicle.<sup>[57–59]</sup> Therefore, ambient vibration is another way for identifying the dynamic properties of a bridge/bridge component. It is especially suitable for measuring the dynamic responses of old bridges which are difficult to work with forced vibration instruments. For the comparison, both excitation methods **T1** are summarized in Table 1.

### 3 | LABORATORY AND FIELD TESTS

Bridge scour detection using the natural frequency spectrum of a bridge/bridge component has been validated by laboratory and field tests. Various sensors have been installed in laboratory models and *in situ* tests to record dynamic data. These studies are presented below in chronological sequence.

Shinoda et al.<sup>[52]</sup> evaluated the performance of a bridge pier after riverbed degradation using forced vibration tests in both a laboratory and the field. In the laboratory test, a velocity sensor was installed at a location very close to the top of the pier to record dynamic data. The vibration was generated by hitting the plane that the velocity sensor is fixed on using an iron ball. Different contact durations between the iron ball and pier were measured in the laboratory test. It was concluded that the minimum contact duration should be applied to separate the iron ball-induced frequency from the pier PNF. In the field test, a bridge pier was studied using the same method as that in the laboratory to detect the PNF of the pier after riverbed degradation. The measured PNF was compared with the PNF in a condition without scour, which was calculated using an experimental formula. The results from the field test confirmed that the PNF of the bridge pier decreased with the damage of the pier and increased with

reinforcements. The results did not explicitly point out the relationship between bridge scour and the PNF of the pier. However, the riverbed degradation indicated that scour-induced damage was the main reason.

Masui et al.<sup>[60]</sup> developed a soundness evaluation system to detect bridge scour based on ambient vibration measurements. Vibration sources were derived from passing trains and floods. A servo acceleration sensor was installed on the top of a pier and used to collect vibration wave shapes via wireless LAN. Different evaluation indicators were proposed and utilized to identify the pier integrity separately. Train-induced vibration was evaluated using the ratio ( $\beta$  = horizontal acceleration amplitude/vertical acceleration amplitude) of horizontal root mean square (RMS) to vertical RMS, while flood-induced vibration was estimated using the PNF of the pier. For the train-induced vibration, a passing train mainly induced vertical vibration, while horizontal vibration tended to increase as bridge scour developed. In that case, the value of  $\beta$  increased with scour development because, when a train passed, the horizontal RMS increased while the vertical RMS remained unchanged. This theory was validated by comparing  $\beta$  in the scoured pier and the unscoured pier in the field test. The results confirmed that calculated  $\beta$  in the scoured pier was greater than that in the unscoured pier. For the flood-induced vibration, the dynamic responses of the pier caused by a micro-tremor under floods were recorded using the same acceleration sensor. Then the PNF of the pier was calculated by transferring recorded data using FFT. After that, the PNF under floods was compared with the previous PNF. This comparison validated that the change in the PNF of a pier can be used to evaluate scour conditions.

Yao et al.<sup>[53]</sup> used the PNF of a bridge pier to experimentally study scour development by employing multiple sensors at a shallow foundation. To simulate the real superstructure, a concrete column with a diameter of 0.45 m and a length of 4 m was used to simulate the pier as shown in Figure 3a. Two prefabricated concrete decks were installed end-to-end on the top of the column to simulate bridge decks. The concrete column was embedded into a sand matrix in a 2D flume to simulate a shallow foundation. Various sensors were set up to record experimental data, including a motion sensor, a tilt sensor, a float out device, a water stage sensor, a sonar sensor, an Acoustic Doppler Velocimetry, and a Tethered Buried Switch instrument. The motion sensor was installed on the top of the pier to record dynamic responses of the pier (Figure 3a). The test was performed in several steps. Firstly,

**TABLE 1** Comparison of excitation methods

Excitation types	Vibration sources	Advantages	Limitations
Forced vibration	Vibrator oscillator, hammer, iron ball, etc.	High DF/UF ratio, known input function, easy data identification	Low safety, traffic interruption, high cost in field tests, time and labors waste
Ambient vibration	Winds, floods, passing vehicles, etc.	Economical in time/labor, high safety	High UF/DF ratio, unknown input function, difficult data post-processing

Note. DF/UF = desired frequency to undesired frequency.

a hammer was used to generate vibration when the flume was not filled with water. Then the flume was filled with water and vibration was generated by a flow, in which different flow velocities were implemented. A bridge scour hole was developed as the flow velocity increased. The experimental results presented in Figure 2 indicate that the first three natural frequencies of the simulated pier in the flow direction (scour-preferred direction) decreased with time as soon as the scour hole developed. The frequencies continued decreasing as the scour depth increased. In a subsequent study, *in situ* scour detection tests of two bridges in Texas were conducted using the same instruments in the laboratory test.<sup>[61]</sup> The motion sensor was glued to the cap beam to record the dynamic responses of the bridges. Vibration was generated by a passing vehicle. By analyzing the measured data, it was found that there was a difficulty in obtaining the PNF due to the discontinuous measured acceleration signals, which was due to undesired noises and the power shortage at the sensor during the tests.

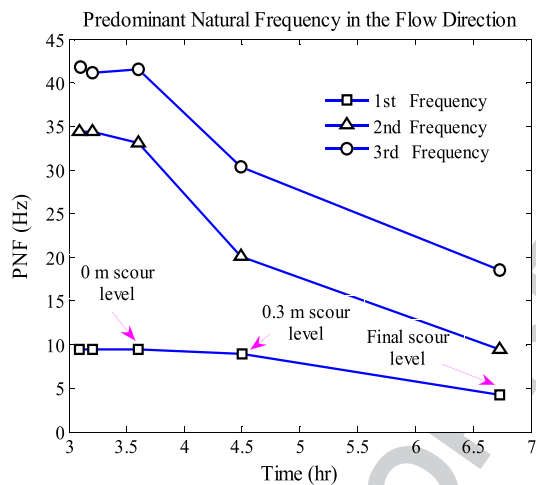


**FIGURE 2** Variation of the predominant natural frequency (PNF) in the flow direction [Reproduced from Yao et al.<sup>[53]</sup>]

Briaud et al.<sup>[62]</sup> continued to refine the previous laboratory model<sup>[53]</sup> to investigate the PNF-bridge scour relationship in a deep foundation in addition to the shallow foundation. As shown in Figure 3b, eight rebars as piles were installed into the bottom of the concrete column to simulate the deep foundation combining a bridge pier and a pile foundation. The model for both the shallow and deep foundations followed the same procedures as that used in Yao et al.<sup>[53]</sup> A bridge scour hole developed with the increase of the flow velocity. When the scour hole reached the bottom of the pier or the piles, the pier started to settle and rock. A conical shape scour hole was formed in experiments for both foundations. A motion sensor was installed at the top of the pier to record the dynamic responses of the pier. The experimental results of the shallow foundation demonstrated that the first natural frequency of the pier in the flow direction (scour preferred direction) decreased from 9.5 Hz to less than 4 Hz within 3 hr. This was the time when scour depth continuously increased. The second and third natural frequency of the pier in the flow direction greatly decreased as well. However, the first natural frequency of the pier in the traffic direction almost remained unchanged during the period. A similar result was obtained for the deep foundation model, though the decrease in the first natural frequency was smaller at the beginning of the scour hole development. All results indicated that the PNF of the pier in the flow direction decreased as the scour depth increased.

Ko et al.<sup>[49]</sup> proposed a set-up of field measurements on bridges and the schemes of data processing to accurately detect scour using the natural frequency spectrum in the field test. Two *in situ* cases were investigated to examine how bridge scour affects the dynamic responses of bridge piers. One was bridge piers with severe scour (6–7 m) and slight scour (0.5–1 m). The other was a bridge pier with 4.5- and 7.5-m scour level. The vibration source was a passing vehicle. Dynamic data in the two cases were recorded using velocity sensors. But the locations of the sensor installation were different. The sensors were installed on the cap beam

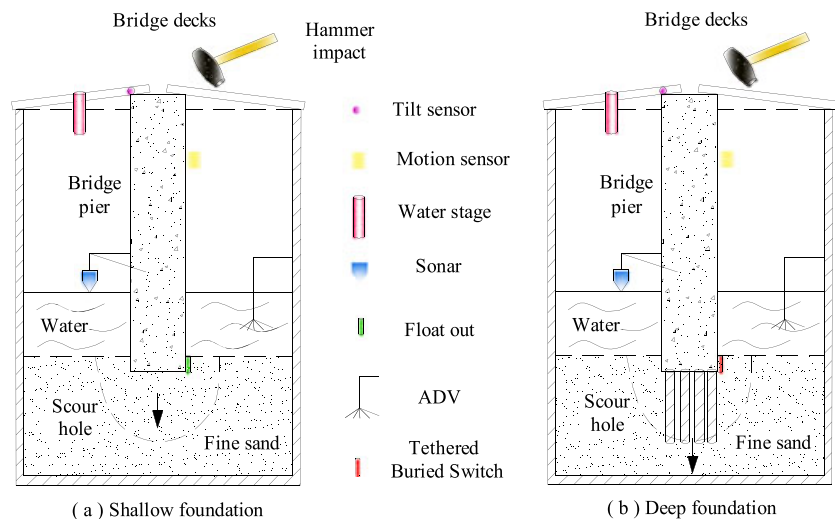


**FIGURE 3** Schematic of the scour tests in the shallow foundation (a) and deep foundation (b) [Reproduced from Briaud et al.<sup>[62]</sup>]

in one case, while in the other case, the sensors were installed on the one side of a bridge deck. The difference in the PNF of the pier was evaluated by comparing the cases under slight and severe scour conditions. The schemes of data processing were utilized to obtain a representative PNF by averaging FFT natural frequencies of three recording sections extracted from the overall recording. Details of the post-data processing will be later introduced in the 5 Section. The results revealed that the change in the PNF of the pier was negligible in the traffic direction due to the constraint from decks. However, the PNF of the pier explicitly decreased in the flow direction as scour depth increased. The reason was that the overall stiffness of the tested pier was decreased due to scour development. This was mostly true in the flow direction because scour was induced by the flow.

The influence of soil strength and water level on the natural frequency spectrum of a bridge pier was experimentally investigated with ambient vibration.<sup>[63]</sup> As shown in Figure 4, a single bridge pier with different penetration depths was used to simulate different scour situations in the laboratory. To investigate the effect of the soil strength, two soil blocks with different compression strengths were measured. Three vibration sensors were used to record dynamic signals of the pier, among which two sensors were installed on the top of the pier (top sensor) and the other one was on the soil surface layer near the pier (bottom sensor). To obtain a better interpretation, this study introduced two indicators. One was the PNF,  $f_{imp}$ , measured from the impact by the flood. The other was the value of  $f_{mi}$ , which was the ratio of the PNFs measured by the top sensor to that by the bottom sensor. The results indicated that the values of both  $f_{imp}$  and  $f_{mi}$  decreased regardless of the compression strength of the

soil blocks. The maximum reductions in the  $f_{imp}$  and  $f_{mi}$  in the same soil block were approximately 80% and 60%, respectively. In addition, the relationship between the water level and the fluctuation of the pier PNF measured using microtremors was studied. The ratio ( $r_{wp}$ ) of the water level to the pier height was chosen for evaluation. This pier height was the distance from the top of the pier to the soil surface, which thus excluded the embedded part in the soil. The ratio ( $r_{mi}$ ) between the PNF measured using microtremors to that measured using impact vibration was also selected in this study. If  $r_{mi}$  was equal to one, the PNF measured using microtremors was equivalent to that measured using impact vibration. The relationship between these two ratios, that is,  $r_{wp}$  and  $r_{mi}$ , was investigated. It was concluded that it was better to identify the PNF of the pier was at high water levels. This was because most measured PNFs tended to converge to the measured PNF using impact vibration at greater water levels.

The quality of dynamic data collection for scour detection was evaluated with a field test on a real bridge using wireless sensor networks.<sup>[64]</sup> The field test was conducted at an actual bridge with two piers. The wireless sensor system was assembled based on the Imote2.NET to include ITS400, Imote2, data acquisition, sensor module, microprocessor, and wireless RF module. Three Imote2-based sensing nodes were installed on the top, center, and bottom of the test bridge pier to collect the dynamic responses generated by force vibration. The acceleration responses and the PNFs of two scour scenarios, that is, no scour depth and 4 m scour depth, were collected and compared. It was found that the acceleration responses of the test pier collected from the top, center and bottom of the pier were clear enough for scour detection. The PNFs measured from the top of the pier also clearly showed the difference between the PNFs of no scour depth and those of 4-m scour depth. The field test results confirmed good-quality data collection on a real bridge for scour detection using the PNFs.

Foti and Sabia<sup>[65]</sup> investigated the change in the modal identification of bridge spans and in the dynamic signals under the influence of scour in the field. The riverbed level in the measured bridge was decreased after a flood event, which resulted in a 6-m deep scour hole around one of the bridge piers. After that, this scoured pier was retrofitted with a new foundation mat. To evaluate the retrofitting, two different evaluation approaches were applied when comparing the dynamic responses of the bridge with scour to that after retrofitting. One approach was the modal identification of bridge spans by comparing mode shapes and corresponding frequencies of bridge spans before and after retrofitting. Figure 5a shows the results of the modal identification of the bridge spans, in which the mode shapes and the corresponding frequencies of Mode 1 and Mode 3 for the bridge spans before and after retrofitting are presented respectively. The results of Mode 1 presented in Figure 5a(1) indicates that the anomalous mode shape and lower frequency

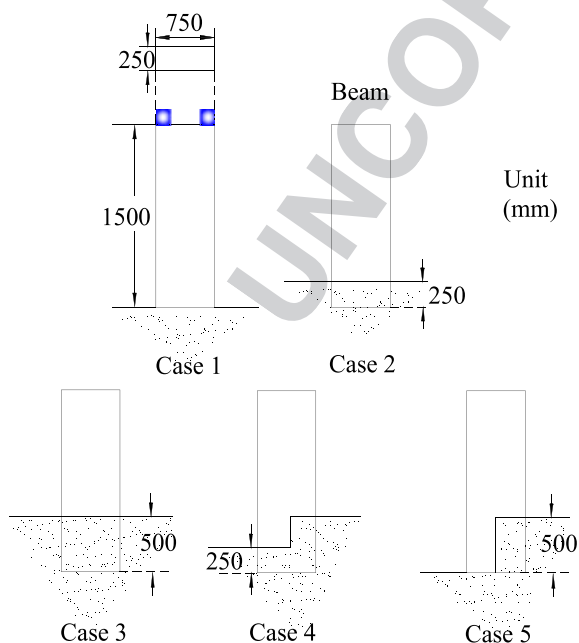
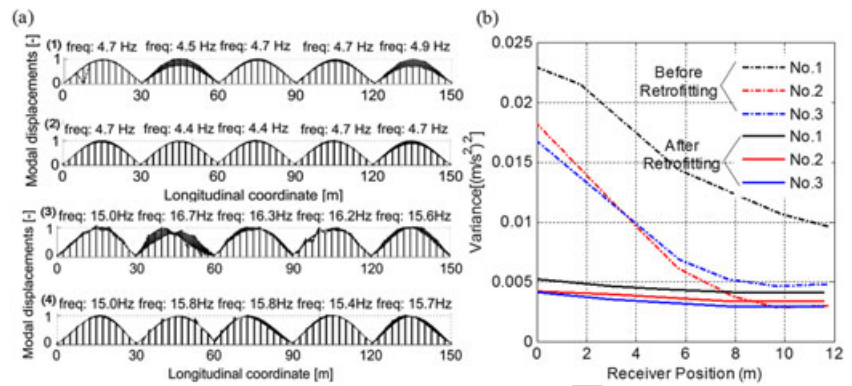


FIGURE 4 Schematic of different scour test situations [Reproduced from Samizo et al.<sup>[63]</sup>]



**FIGURE 5** Results of experimental tests: (a) mode shapes and corresponding frequencies of: Mode 1 for bridge spans (1) before retrofitting and (2) after retrofitting; Mode 3 for bridge spans (3) before retrofitting and (4) after retrofitting; (b) dynamic responses of the scoured pier under three different passing vehicles [Reproduced from Foti and Sabia<sup>[65]</sup>]

appeared in the second span, which was supported by the scoured pier, when compared with the other spans before retrofitting. But the mode shape and the frequency of the second span became normal after retrofitting. The conclusion regarding whether the anomalous difference was due to scour was questionable because this anomalous difference in the second span may be attributed to defects in the span itself. This issue was addressed by comparing the results of Mode 3, which confirmed that the anomalous mode shape and the lower frequency were caused by scour because the frequency in Mode 3 was greater than the other spans before retrofitting as shown in Figure 5a(3). The mode shape of the second span became more regular and its frequency approximated to the other spans after retrofitting, which also validated the interpretation of the anomalous difference in the second span caused by scour (Figure 5a(4)). The other approach was the observation of the dynamic response of the scoured pier by comparing the dynamic responses of observing points on the foundation mat before and after retrofitting. The observing points were distributed from upstream to downstream. The vibration was generated by a passing vehicle. Three experiments were conducted using different vehicles before and after retrofitting, respectively. Data were collected with accelerometers and a dynamic signal acquisition device. The results of the dynamic responses are presented in Figure 5b, which presents a plot of the diagonal terms of the covariance matrix calculated for the dynamic signals from the observing points of the scoured pier before (dashed lines) and after (solid lines) retrofitting. It can be shown that the variances of the scoured pier before retrofitting were significantly different from that after retrofitting for all three tests.

Similar results were observed in another laboratory study with the discussion on the impact of water on the measured PNF.<sup>[54]</sup> The laboratory model used a steel square hollow beam to simulate a pier. The vibration was generated by an impulse hammer hitting. Uniaxial accelerometers were installed on the top of the pier to record dynamic data. The simulated pier was installed in a sand matrix with 100% relative compacted density. To simulate different bridge scour depths, the sand was removed in five identical increments for each level. The experimental results showed that obvious

reductions occurred in the PNF of the simulated pier between any two scour levels (Figure 8a). Then, a field test was performed using the same procedures. Soil samples were comprised of a very dense and fine sand deposit, which was a better *in situ* site conditions when compared with that in the laboratory. The results showed that the PNF decreased as scour depth increased. However, the models neglecting the effect of water did not reflect the *in situ* condition of piers if a pier was always submerged under water. Hence, another experiment was designed to assess the effect of water level on the PNF. Three cantilevers with different geometries were used as piers. The effect of water was evaluated by comparing the variation of the PNF in air and in water separately. The experimental results indicated that the presence of water affected the PNF of the flexible piers much more than that of the stiff ones. However, the PNF of a pier with a high stiffness vibrating in air was very close to that in water. The influence of water on the PNF was also discussed in Lin and Wang.<sup>[66]</sup> A series of static experiments was conducted with a single pier. Three velocity meters were installed on the top of the bridge pier to record the dynamic responses. The measured PNFs with different combinations of the imbedded pier length and water level were compared. The test results indicated that the imbedded pier length had a significant effect on the measured PNF, while the influence of water on the measured PNF was minor.

The performance of PNF-based scour detection was further investigated with experiments to represent a more realistic bridge situation.<sup>[67]</sup> Concrete pier models were chosen in 1/36 proportion of the Chun-Sha Bridge piers to include caisson foundations (49-cm length), piers (23-cm length), and pier caps. The pier models were imbedded in a straight line in the channel. Sands were paved in the channel to reflect the actual situation. Water was included in this experiment, and the flow rate was selected based on the actual flow rate measured from the river where the Chun-Sha Bridge is located. Accelerometers were installed on the top of the test piers to collect dynamic data from two directions, that is, the flow direction and the direction that is perpendicular to the flow direction on the same plane. The collected data were transmitted to a computer using wireless sensor network for data post-processing. The experimental results clearly

showed that the PNFs measured from these two directions decreased as scour developed.

To conclude, a bridge pier is the preferable test component in the previous experimental tests. A sensor such as a velocity sensor or an accelerometer is frequently deployed on the pier body to collect dynamic signals due to the simple installation and good signals pick-up. In most cases, scour holes are symmetrical as soils around the pier are removed by equal layers. The selected soils are erodible for the purpose of easily forming scour holes within a short time during the tests. All details of the studies presented above are summarized in Table 2. Experimental investigations indicate that the PNF can be an indicator of bridge scour detection. Therefore, identifying the natural frequency spectrum of a bridge or a bridge component allows inspectors to evaluate the evolution of the scour hole and the bridge integrity. The PNF is dependent on the stiffness of the foundation systems. If a bridge scour hole develops, the system stiffness decreases; accordingly, the PNF decreases. Hence, bridge scour detection can be taken in real-time monitoring using the natural frequency spectrum.

#### 4 | NUMERICAL STUDIES

The idea of the PNF-based scour detection has also been explored using numerical methods such as finite element models (FEMs). Due to the different experiment types, the numerical models can be classified into two categories, that is, models for simulating laboratory processes and those for field-scale tests. The two categories are introduced separately in chronological order. Numerical results are usually compared with the results from either laboratory or field tests to validate the numerical models.

#### 4.1 | Simulations for field-scale models

A numerical model was developed by Foti and Sabia<sup>[65]</sup> to evaluate bridge scour with focus on the difference in the dynamic responses and the influence of load positions. A single pier, which supported two bridge spans, was modeled in a FEM. Pile foundations were reproduced using 3D beam elements. The interaction between the pile and the surrounding soils was modeled with distributed vertical and horizontal springs.<sup>[68,69]</sup> The springs were assumed to be linearly elastic. Scour situations were modeled by suppressing springs at the top portion of pile foundations. Therefore, more rows of springs were suppressed to simulate different scour depths. To obtain the dynamic responses of the pier, a triangular impulse was used as an external excitation. The numerical study showed that there was a distinct change in the dynamic signals at different scour depths. In addition, to avoid the confusion, the influences of the different external load positions were studied using the same numerical model. A load applied on the downstream side of the pier (the same side of the scour hole) and on the upstream side separately. The numerical results revealed that different external load positions induced the different absolute values of the dynamic signals variances, which was the diagonal terms of the covariance matrix calculated for the observing points of the pier. Though the PNF-scour relationship was not presented directly, this study provided the evidence of identifying scour damage using the dynamic responses of a pier.

An integrated model combining genetic algorithms was developed to determine the PNF of a bridge from numerous frequencies calculated by the modal analysis.<sup>[70]</sup> This model used the effective mass above the soil surface to determine the PNF of the bridge.<sup>[71]</sup> They defined the effective mass ratio as the ratio of the mass above the soil surface to the total mass in a certain direction with a specific degree of freedom,

TABLE 2 A summary of laboratory and field tests

Test component(s)	Instruments	Vibration types	Scour shape	Soil properties	Sensor location
<i>In situ</i> caisson pier <sup>[52]</sup>	Velocity sensor	Forced	No	—	Top of pier
<i>In situ</i> pier <sup>[60]</sup>	Sevo accelerometer	Ambient	No	—	Top of pier
<i>In situ</i> pier/deck <sup>[65]</sup>	A dynamic signal acquisition device, accelerometers	Ambient	Yes	Soft/silty clay	—
Concrete column <sup>[53,62]</sup>	Motion, tilt, sonar, water stage sensor, float out device, TBS device, ADC device	Forced/ambient	No	High erosive soil	Top of pier
<i>In situ</i> pier <sup>[61]</sup>	Motion, tilt, sonar, water stage sensor, float out device, TBS device, ADC device	Ambient	No	—	Cap beam
<i>In situ</i> caisson pier <sup>[49]</sup>	Velocity sensor	Ambient	Yes	—	Cap beam and bridge deck
Concrete pier <sup>[63]</sup>	Vibration sensor	Ambient	Yes	Crushed stone	Top and bottom of pier
Steel cantilever/circular tube <sup>[54]</sup>	Uniaxial accelerometer	Forced	No	High density sand	Top of pier
<i>In situ</i> pier <sup>[64]</sup>	Imote2.NET	Forced	No	—	Top, center, and bottom of pier
Plastic tube <sup>[66]</sup>	Velocity sensor	Ambient	No	Sand	Top of pier
Small-scale real pier <sup>[67]</sup>	Accelerometer, GPS, sensor circuit board, wireless sensor network	Ambient	No	Sand	Top of pier



which could be used as an indicator to determine the PNF from coupled numerical models. This was because the mode shapes of soils, piers, and bridges were coupled together. It was difficult to find out if a predominant mode shape belonged to the bridges or the soils. If the value of effective mass ratio of one mode shape was larger than 30%, this mode can be categorized as a dominant mode shape in that direction. To examine the accuracy, the multispan bridge supported by simple beams were modeled using the FEM.<sup>[72]</sup> By setting different scour depths under different environmental conditions, the possible PNFs of the bridge were calculated. To analyze the considerable number of data generated by the FEM, genetic algorithms were applied to find the fitted generic formula. For the purpose, the relationship among the scour depth, the PNF, and various environmental variables was firstly defined. Then optimal solutions were constructed to be the best fit to this relationship.<sup>[73,74]</sup> The simulations included three pier types, six soil strength, and nine scour depths to investigate their effects on the PNF. By setting optimal fitting formulas, the mean errors for two cases with different types of pile arrangements were 1.1801 and 0.5274 m, respectively, which were acceptable.

The effect of soil strength on the PNF of a bridge was further discussed based on the previous integrated model.<sup>[75]</sup> The modeling process was the same as that in the previous model.<sup>[70,72]</sup> But the focus of this study was a sensitivity analysis of the effect of different soil strength on the PNF of a bridge. To address this issue, six types of soils with different soil strength were adopted in the simulations to show the scour depth-PNF relationship at different scour depths. For Types 1 to 4, the Young's modulus of soil linearly increased with the soil depth from the top of the soil to the bottom. In contrast, the modulus linearly decreased with the soil depth for Type 6 while the modulus remained unchanged for Type 5. The simulation results showed that the PNF of the bridge decreased with an increase in the scour depth in all cases (Figure 12a). However, the numerical results indicated that the soil strength had a negligible impact on the PNF of the bridge (Figure 12a). This was particularly true when the progression of scour depths was from 0 to 6 m. During this period, the PNF was almost unchanged.

Zhang et al.<sup>[76]</sup> constructed a FEM to find out the relationship between the scour depth and the PNF of a bridge with focus on the influence of the pile length and the soil strength. To avoid confusion, the bridge superstructures were assumed to remain unchanged for all analyses. The key variable was the difference in the bridge foundations affected by scour. The purpose was to find out the influences of the scour depth on the PNF of the bridge. Issues regarding how the pile arrangement and the soil strength affected the PNF were discussed by investigating different pile lengths and soil strengths. The boundary conditions of soils were restricted except in the top surface layer. The numerical results concluded that the PNF of the bridge decreased with an increase in the scour depth. Also, different lengths of the pile and the soil strength would affect the PNF of the bridge. The PNF increased with the increase of the pile length. However, the difference in the PNF calculated with different pile lengths was smaller if the soil strength was high when compared to that with low soil strength. The PNFs were very different if the soil strength differed. The PNF increased with the increase of the soil strength, regardless of the pile length.

A numerical model of a full-scale bridge had been developed by considering more parameters to focus on determination of the PNF of a scoured bridge with the SSI.<sup>[77]</sup> For most bridges, there were primarily two types of interactions, that is, SSI and fluid–structure interaction (FSI). Effects of both of them on the PNF of the scoured bridge were studied and analyzed separately. For SSI, the dimensions of the soil mesh were chosen to be over twice of the foundation dimensions in the horizontal plane to better represent the soil–structure behavior. The model also adopted the effective mass of the full-scale bridge above the soil surface to determine the PNF. The critical issue was to identify the predominant mode shape of the bridge. The first step was to find the value of the effective mass ratio of one mode shape that was greater than 30% to be the predominant mode shape, following the same procedure used in Feng et al.<sup>[70]</sup> As shown in Figure 6, the PNF of the bridge decreased with an increase in scour depths in both the bridge longitudinal and the transverse directions, but the decrease was not smooth due to the nonuniform cross-sections of the foundation. In addition, this decreased

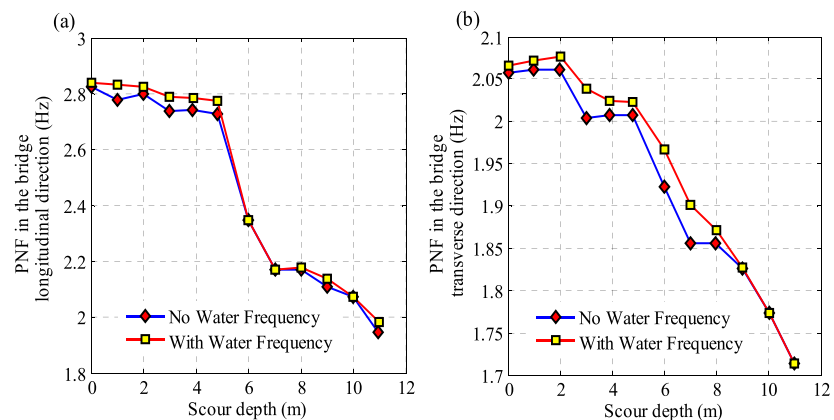


**FIGURE 6** Variation of the predominant natural frequency (PNF) of the bridge with scour depth: (a) PNF variation in the bridge longitudinal direction; (b) PNF variation in the bridge transverse direction [Reproduced from Ju<sup>[77]</sup>]

trend was more obvious if the scour depths were below the bottom of the pile cap. For the FSI, the formulation of a compressible and inviscid fluid at a small velocity was employed. The fluid velocity, the bulk modulus, and the fluid mass density were considered. The numerical results led to the conclusions that the calculated PNF without water was always higher than that with water, as presented in Figure 6. However, the effect of fluids on the PNF of the bridge seemed to be negligible because the difference between the PNFs considering and without considering water was less than 1% in both directions. Notwithstanding, the fluid effect might increase if all the bridge foundations, including piles, pier caps and piers, were submerged into water when water level was extremely high.

A more complicated cable-stayed bridge was modeled to determine the scour status for a pier of this full-scale bridge using the natural frequencies of the bridge.<sup>[78]</sup> The natural frequencies used in this study consisted of vertically flexural frequencies, horizontally flexural frequencies, axial frequencies, and torsional frequencies. The support of this cable-stayed bridge included a pylon at the location close to the middle of the whole bridge span, an abutment at the left-end side, and a bridge pier at the right-end side. Because of the complicity of modeling this cable-stayed bridge, four steps were made to determine the scour status for the right bridge pier. First, a simplified model, neglecting the left abutment and the right bridge pier, was developed and validated against the field test results by modifying the boundary conditions to obtain a good accuracy. Second, a comprehensive model was developed by adding the right bridge pier. Third, the optimal soil stiffness was estimated for the right bridge pier by fitting the critical bridge natural frequencies using a known soil deposit at the pylon. Finally, scour status for the right bridge pier was determined using the optimal soil depth to fit the two sensitive frequencies of this bridge pier. The determined scour depth was validated against a practical scour measurement, for which an agreement was obtained. This study confirmed that the natural frequency spectrum-based scour detection was also feasible for complicated bridge types such as cable-stayed bridges.

#### 4.2 | Simulations for lab-scale models

Briaud et al.<sup>[62]</sup> conducted a three-dimensional (3D) FEM to identify the PNF of a bridge pier with emphasis on how the PNF changed in the flow and the traffic directions. Two types of foundations, that is, shallow and deep foundations, were modeled and analyzed separately. For simplicity, water was not included. In the shallow foundation model, a single pier that supported two bridge decks was embedded in the soil block. All the material properties were taken from either field tests or manufacturer specifications. To model the contacts between different elements, normal interface springs were employed between all penetrating nodes and on the contact surfaces such as the pier–soil surface. The presence of the

scour hole was simulated by changing the contour of the mesh along the soil surface. The scour depth was changed in increments of one-third of the total embedment of the pier to simulate four different scour depths: 0, 0.1, 0.2, and 0.3 m. The PNF of the pier was obtained directly from modal analysis. In the deep foundation model, all the parameters and procedures were identical to the shallow foundation model except that eight piles were placed under the bottom of the pier. As shown in Figure 7, the numerical results shows that the PNF of the pier decreased with the development of a scour hole in the flow direction in both the shallow and the deep foundation models. The numerical solutions were close to the experimental values. However, the PNF in the traffic direction almost remained unchanged.

Prendergast et al.<sup>[54]</sup> developed a simple FEM to investigate the way to determine the stiffness of springs for the soil–structure interaction using the natural frequency spectrum for scour detection. Both a laboratory and a field test were modeled to investigate the change in the pier PNF due to the scour development. For simplicity, a single pile was utilized to simulate a pier, which was modeled using beam elements. A series of horizontal springs was used to model the interaction between the pier and the soils around the pier. The scour process was simulated by progressively removing the springs from the top downward. To obtain correct numerical results, it was critical to assign the stiffness values to the springs so that the lateral stiffness of the soils around the pier could be accurately represented. Two approaches were employed to determine the lateral spring stiffness values. The small-strain stiffness (SSS) measurement utilized the small-strain modulus, which was obtained using shear wave velocity measurements or Ten Cone Penetration Tests, to represent the lateral stiffness of soils. The American Petroleum Institute method to determine the lateral stiffness of soils was based on a Winkler model by calculating the secant modulus of the lateral force-lateral displacement curve. The results of the lab-scale simulations shown in Figure 8a demonstrate that there was an explicit reduction in the pier

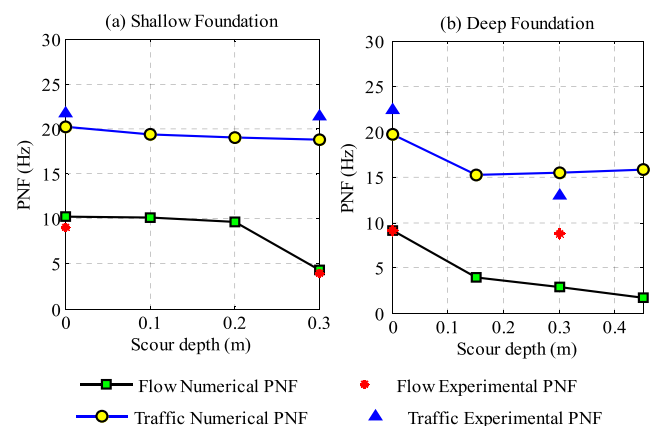


**FIGURE 7** Predominant natural frequency (PNF) changes with scour depths in the shallow foundation and deep foundations [Reproduced from Briaud et al.<sup>[62]</sup>]

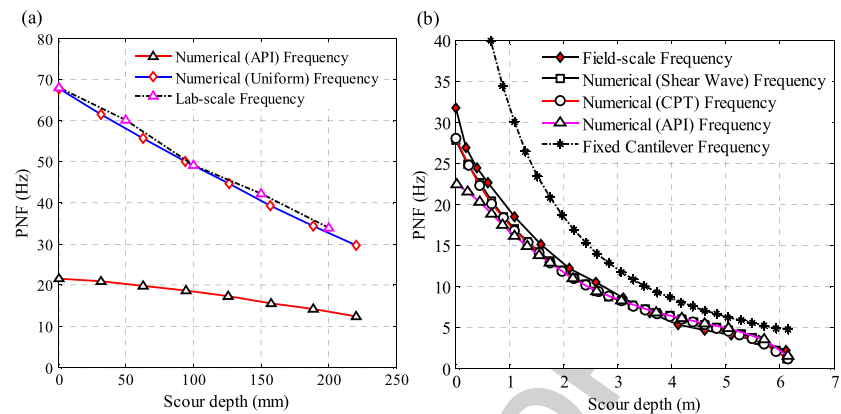


**FIGURE 8** Variation of the predominant natural frequency (PNF) with scour depth in numerical and experimental PNF: (a) lab-scale results comparison; (b) field-scale results comparison [Reproduced from Prendergast et al.<sup>[54]</sup>]

PNF from a mildly scour condition to a serious scour condition. The SSS performed very well when compared with the PNF observed experimentally. However, the APT either underestimated the PNF at smaller depths of scour or overestimated slightly at greater scour depths. The main reason was that the nonuniform stiffness profile for the model could not reflect the stiffness of the soils in the laboratory test. The *in situ* stiffness of the soils depended on the sand density and mean stress level.<sup>[79]</sup> The soils used in the laboratory test were compacted during the test. This procedure led to a high lateral stress and a high relative density. As a result, a uniform stiffness values profile for spring-beam models were more accurate for the laboratory test. Besides the lab-scale simulations, a field-scale simulation was conducted using the identical process. For comparisons, the two approaches to determine the lateral stiffness of soils were plotted to compare with the field data. The frequency variation of a fixed cantilever with respect to scour development was also presented. As shown in Figure 8b, the PNF decreased as the scour hole developed in which all numerical PNF was in good agreement with the experimental PNF. But there was a larger deviation for the APT at the beginning of scour progression when compared to others.

In conclusion, both modal analysis and dynamic analysis have been used to obtain the PNF for scour detection. Parameters such as the SSI and the pier length have been comparatively discussed. The results regarding the effect of water indicate that the FSI was negligible due to small deviations. But the fluid effect might increase if all the bridge foundations were submerged into water. The issue regarding the way to determine the stiffness of soils using springs to represent the SSI was investigated, which highlighted the difference in determining the stiffness of soils in the lab-scale test and the field-scale test. The details are summarized in

T3 Table 3.

## 5 | DATA PROCESSING SCHEMES

Data processing schemes are introduced regarding the methods for processing the data collected from the transient response and the modal analysis. The schemes of the

transient response are based on FFT for determining the PNF from numerous dynamic signals. For the modal analysis, new parameters are defined to identify bridge scour by evaluating the change in the new parameters. Details of schemes are presented in the following subsections based on different data sources, that is, experimental tests and numerical calculations.

### 5.1 | Data from laboratory and field tests

Different indicators were used in laboratory and field tests for the data processing. One significant indicator is the PNF. FFT has been extensively used to identify the PNF. The integrity of a bridge or a pier can be evaluated directly by examining the change in the PNF.<sup>[52–54,61,62]</sup> Another popular indicator is the ratio between the transversal RMS and the vertical RMS,<sup>[60,61]</sup> which utilizes the change in this ratio to monitor scour development. Specific schemes used in these studies will also be introduced.

Shinoda et al.<sup>[52]</sup> utilized FFT by transforming dynamic signals from the time domain into the frequency domain to identify the PNF of the bridge pier. To assess the pier performance, a ratio was introduced by comparing the identified PNF to a reference PNF calculated from an empirical equation as Equation (2):

$$F = 11.83 \times \frac{N^{0.184}}{W_h^{0.285} \times H_k^{0.059}} \quad (2)$$

where  $F$  (Hz) is the standard PNF;  $N$  is the number obtained with the standard penetration test;  $W_h$  (N) is the weight of superstructure;  $H_k$  (m) is the height of the pier minus the height of the slab on the top of the pier. This ratio can reflect the variation of the PNF, with which scour scenarios could be evaluated. To easily examine the integrity, this study proposed four evaluation criteria, that is, 0–0.70, 0.70–0.85, 0.85–1.00, and greater than 1.00, which represents severe damage, slight damage, fair, and good performance, respectively. The value of this ratio can be directly used to evaluate scour conditions.

Masui and Suzuki<sup>[60]</sup> defined a parameter to process train-induced dynamic data. The ratio of the transversal

TABLE 3 A summary of numerical models

Structure configurations	Scour depth	Pier length/pile arrangement	Scour shape	FSI	SSI
Single pier with two spans and 24 piles <sup>[65]</sup>	Yes	No/No	No	No	Spring-beam
Single pier with two desks <sup>[62]</sup>	Yes	No/No	No	Yes	Soil-pier
Full-scale bridge <sup>[70,72,75]</sup>	Yes	Yes/Yes	Yes	No	Soil-pier
Full-scale bridge <sup>[76]</sup>	Yes	Yes/Yes	No	No	Soil-pier
Single pile <sup>[54]</sup>	Yes	No/No	No	Yes	Spring-beam
Full-scale bridge <sup>[77]</sup>	Yes	No/No	No	Yes	Soil-pier
Full scale cable-stayed bridge <sup>[78]</sup>	Yes	No/No	No	No	Spring-beam

Note. FSI = fluid–structure interaction; SSI = soil–structure interaction.

RMS to the vertical RMS, which was defined as  $\beta$ , was used. The principle of this technique is that passing trains primarily cause a bridge pier to vibrate in the vertical direction rather than in the transversal direction. However, the development of bridge scour leads to large changes in the transversal vibration. Hence, if the value  $\beta$  in conditions without scour is known, any changes in the rigidity of the pier indicate that bridge scour develops. An increase in the value of the transversal RMS results in a decrease in  $\beta$ . However, a slight change in  $\beta$  does not mean that scour around bridge foundations develops, because this change in  $\beta$  can also be attributed to deviations in the field measurements. If  $\beta$  locates within a

normal range calculated from statistical evaluation, the effect of scour is negligible. Otherwise, scour tends to be severe due to a decrease in the pier rigidity.

Masui and Suzuki<sup>[60]</sup> and Ko et al.<sup>[49]</sup> proposed a method based on FFT to identify the PNF from numerous measured data by flood-induced vibration. This method is used to accurately extract the PNF from the measured data caused by flood-induced microtremors. For the purpose, collected dynamic data are divided into three parts shown in Figure 9 (a), for example,  $f_1$ ,  $f_2$ , and  $f_3$ , in which each part is partially overlapped with the next. The calculation process is shown in Figure 9. The FFT of each part is computed firstly. Then the

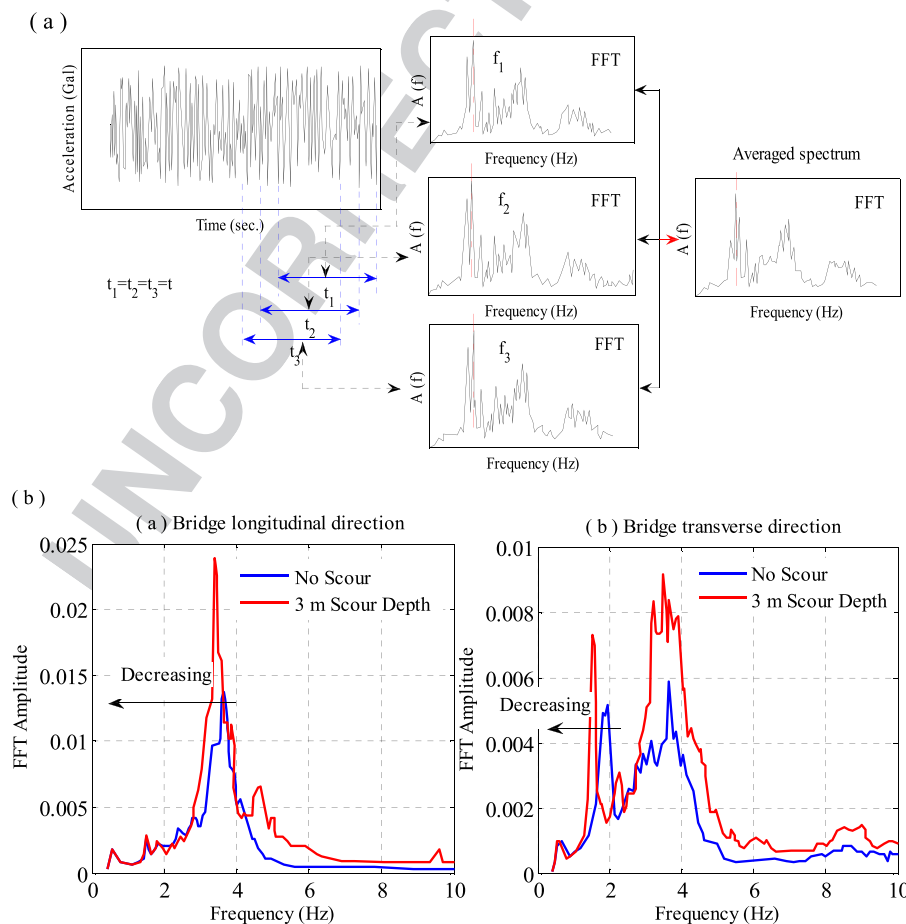


FIGURE 9 Field data processing using Fast Fourier Transform (FFT): (a) calculation of the predominant natural frequency from original collected data [Reproduced from Masui and Suzuki<sup>[60]</sup>] and (b) averaged Fourier spectra of collected data [Reproduced from Ko et al.<sup>[49]</sup>]

accurate PNF can be obtained by overlapping and averaging those parts ( $f_1, f_2, f_3$ ) using Equation (3):

$$F = \frac{\sum_{i=1}^N f_N}{N} \quad (3)$$

where  $F$  (Hz) is the PNF;  $N$  is the number of the division parts;  $f$  (Hz) is the PNF of a division part. The averaged Fourier spectra of collected filed data for a real pier, including vibration of a test pier and ambient vibration, are shown in Figure 9(b). It can be seen that the PNF decreases obviously as scour depth increases.

## 5.2 | Data from numerical calculations

The schemes for processing numerical data/results are summarized in this section. Due to the conclusion that bridge scour affects the predominant mode shape and its corresponding natural frequency of a bridge or a bridge pier, new parameters will be defined based on the modal analysis to examine the integrity of a bridge or a bridge pier in simulations by evaluating the change in the defined parameters. Typical schemes are introduced regarding how to define the new parameters and how to identify the progression of bridge scour using the defined parameters.

Foti and Sabia<sup>[65]</sup> proposed a method to process dynamic signals obtained from their numerical calculations. This method included three main steps. First, signals were band-pass filtered to remove the background noise effect. Then the auto-regressive moving average vector technique was applied to the dataset.<sup>[80–83]</sup> Finally, post-processing was employed to identify possible structural vibration modes. The post-processing also included three steps. Firstly, if a modal damping factor was higher than 10%, the corresponding vibration modes were discarded so that the actual structural modes can be selected. Secondly, the possible structural vibration modes could be selected if the frequencies are close to one of the most recurrent values in previous identified vibration modes. Finally, the natural frequency and modal damping values could be determined by averaging the values corresponding to vibration modes characterized using mutually similar mode shapes. Similar mode shapes during this process are dependent on modal assurance criterion coefficient ( $MAC_{i,j}$ ) in Equation (4):

$$MAC_{i,j} = \frac{|\Phi_i^H \Phi_j|^2}{|\Phi_i^H \Phi_i| \cdot |\Phi_j^H \Phi_j|} \quad (4)$$

where  $H$  is the Hermitian of the vector;  $i$  and  $j$  are the numbers of mode shapes. If  $MAC_{i,j}$  exceeds a predetermined threshold (case dependent), those modes are believed to be similar. Additionally, to exclude unreal solutions, an identified mode shape is retained only if its components are characterized by phase angles close to  $0^\circ$  or  $180^\circ$ . The reliability of the inferred

dynamic parameters can be evaluated by a statistical analysis of the results from repeated calculations of several measurements.

Elsaid and Seracino<sup>[84]</sup> offered an approach to process the results of the modal analysis. The assumption was that bridge scour greatly affects the PNF derived from the dynamic characteristics of the horizontally displaced mode shapes. If a change in the curvature of the horizontally displaced mode shapes was calculated, bridge scour could be detected. The difference in the curvature of the horizontally displaced mode shapes for all modes can be summarized using a damage indicator called curvature damage factor (CDF)<sup>[85]</sup>:

$$CDF = \frac{1}{N} \sum_{i=1}^N |v_{oi}'' - v_{di}''| \quad (5)$$

where  $N$  is the total number of modes to be considered,  $v_o''$  is the mode shape curvature of the intact structure, and  $v_d''$  is that of the damaged structure. The location of the damage was captured by calculating the CDF for the first five horizontally displaced mode shapes. If one CDF value of a mode shape exceeded the threshold line of the CDF, this value could be identified. However, if more than one values passed through the threshold line, the results calculated from the CDF might not be accurate because the values in the vicinity of the threshold line were potential false positives. The potential false positives might contribute to the high-order mode shapes rather than the damage mode shapes. A modified curvature damage factor (MCDF) was then introduced to normalize the effect of the higher order mode shapes:

$$MCDF = \frac{1}{N} \sum_{i=1}^N \left| \frac{v_{oi}'' - v_{di}''}{v_{oi}''} \right| \quad (6)$$

MCDF calculates the average of the absolute ratio of the curvature change for a certain number of mode shapes. Therefore, bridge scour can be evaluated by calculating the CDF and MCDF for the first five horizontally displaced mode shapes.

Lin et al.<sup>[66]</sup> proposed the PNF-based structural health monitoring algorithm using a short time FFT. A quadratic formula was utilized to describe the relationship between the imbedded pier length and the PNF as

$$PNF = a \times ID^2 + b \times ID + c \quad (7)$$

where  $ID$  is the imbedded pier length;  $a$ ,  $b$ , and  $c$  are the coefficients of this quadratic formula. In order to use this quadratic formula for scour detection, one needs to first obtain  $a$ ,  $b$ , and  $c$ . For this purpose, at least three sets of  $ID$ s and PNFs are needed. The first set can be obtained from a practical scour measurement at a real bridge pier. The rest two sets can be obtained from numerical simulations of that bridge pier with zero  $ID$  and a half of the initial  $ID$  of that bridge pier. Then, the imbedded pier length can be estimated using this formula if the PNF is known.

Accordingly, the corresponding scour depth can be evaluated.

In summary, FFT has been extensively used to obtain the PNF of a test component in the experimental tests by analyzing its dynamic signals. The ratio of acceleration RMS was also applied in some cases. For simulations, the modal analysis has been utilized to evaluate scour severity by identifying modal identifications in which different parameters were defined and compared for the purpose. The PNF was given via either FFT or the modal analysis. All documented schemes of data processing are summarized in Table 4.

## 6 | UPDATES ON BRIDGE SCOUR MONITORING SENSORS

Updates on bridge scour monitoring sensors are provided in this section to complement the framework of scour damage detection. Scour detection using the natural frequency spectrum of a bridge/bridge pier provides a new perspective for analyzing the integrity of a bridge or a bridge pier against scour hazards.<sup>[65]</sup> Scour monitoring sensors are an effective component to the framework for scour detection. The operational principles of the sensors are introduced in chronological sequence in the following paragraphs. The advantages of

those new sensors are later compared with each other and with vibration-based scour detection, which are summarized in Table 5.

An ultrasonic sensor was proposed to monitor scour in real time.<sup>[86]</sup> The ultrasonic sensor was installed on a vertically fixed trail that allowed the sensor to move vertically (Figure 10a). The ultrasonic sensor worked on the principle that the ultrasonic pulse is reflected at the boundary between water and soils due to the different acoustic impedance as shown in Figure 10a, inferring that the horizontal distance between the water and soils can be measured if a returning signal is received. The scour depth and width can be detected based on the analysis of returning signals. The feasibility of this sensor has been validated in a laboratory test with reasonable accuracy and reliability. One advantage of this method is that an actual river bed map can possibly be portrayed based on the monitoring data. Other benefits include the immunity to noises, little complex wave pattern interferences, and a high resolution. But disadvantages still remain: (a) this sensor needs enough power to move vertically, and (b) the special tube used in the sensor may be expensive because it requires the high protection and a low interference.

A novel passive sensor, called smart rock, has been designed to monitor bridge scour in real time.<sup>[5,87,88]</sup> Smart rocks with embedded electronics were deployed around

TABLE 4 A summary of data processing from different methods

Test component(s)	Data source	Evaluation index	Data processing
Full-scale bridge <sup>[52]</sup>	Tests	PNF	FFT
Full-scale bridge <sup>[60]</sup>	Tests	PNF	FFT; the ratio of acceleration RMS; average of division parts frequencies
Single pier <sup>[65]</sup>	Tests	Modal identification	Three steps: filtering noises; applying ARMAV technique; post-processing, respectively
Single pile <sup>[61,62]</sup>	Tests	PNF	FFT; the ratio of acceleration RMS
Single pier <sup>[63]</sup>	Tests	PNF	FFT
Full-scale bridge <sup>[70,72,75]</sup>	FEMs	PNF	FFT
Single pier <sup>[49]</sup>	Tests	PNF	FFT; Average of division parts frequencies
A simulated bridge <sup>[84]</sup>	Tests and FEMs	Modal identification	CDF; MCDF
Full-scale bridge <sup>[77]</sup>	FEMs	PNF	FFT
Single pile <sup>[54]</sup>	Tests and FEMs	PNF	FFT
Single pier <sup>[66]</sup>	Tests and FEMs	PNF	FFT; three sets of <i>ID</i> and PNF

Note. ARMAV = auto-regressive moving average vector; CDF = curvature damage factor; FEM = finite element model; FFT = Fast Fourier Transform; MCDF = modified curvature damage factor; PNF = predominant natural frequency.

TABLE 5 Comparison of new scour monitoring sensors

Sensor	Durability	Easy in installation	Accuracy	Cost (versus \$1,000)	Other advantages
Ultrasonic sensor <sup>[86]</sup>	Fair	Fair	Good	High	Portray river bed map; high resolution; immunity to noise and complex wave pattern
Smart Rocks <sup>[5,87,88]</sup>	Good	Good	Good	Low	Small size; immunity to noise, debris, salt, temperature, and complex wave pattern; wireless operation
A new TDR <sup>[89,90]</sup>	Good	Good	Good	Low	Acceptable to harsh field environments; flexible size; larger sensing depth
Underwater wireless acoustic sensors <sup>[91]</sup>	Fair	Good	Good	High	Work well under water; wireless operation
Capacitor sensor <sup>[93]</sup>	Fair	Fair	Fair	Fair	Little disturbance to the structure/soil; Work well in soil and under water
Vibration-based scour detection	Very good	Good	Good	Low	Overwater installation; no difficulties like underwater sensors; applicable to complicated bridge types; easy data processing

Note. The estimated index is referred to Chen et al.<sup>[5]</sup>

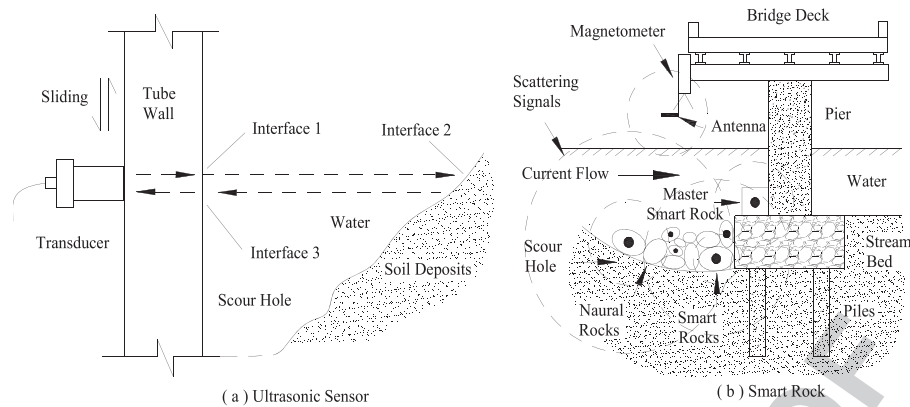


**FIGURE 10** Schematic view of (a) an ultrasonic sensor and (b) smart rocks for scour monitoring [Reproduced from Chen et al. and Wu et al.<sup>[5,86]</sup>]

foundations of existing or new bridges, among which a special sensor, called master smart rock, was tied to the pier cap as a fixed reference point for long term measurements (Figure 10b). Other rocks with different IDs can be deployed into an existing scour hole so that the scour depth can be detected by measuring its disturbance to the Earth's magnetic field with a magnetometer at a remote station (Figure 10b). If the positions of the smart rocks change, the information can be sent using wireless communications to a vicinity mobile station. Smart rocks in the laboratory test demonstrated a good accuracy, but its performance in the field is still being assessed. The primary benefit is that smart rocks always roll into and stay at the bottom of a gradually growing scour hole, which is not affected by extreme events such as a flood. More importantly, both natural rocks and smart rocks protect the bridge pier to the extent. Other advantages include ease of the installation, the high durability, the small size, and the immunity to harsh environments.

A new real-time TDR strip sensor has been developed to monitor bridge scour.<sup>[89]</sup> This sensor works on the principle that the mismatch of materials will result in different

reflections because the electromagnetic wave travels with different speeds in materials with different dielectric spectra. As a result, the huge differences between the dielectric properties of water and sands can be displayed clearly in the time domain signal for scour depth detection.<sup>[89,90]</sup> The accuracy of this sensor was validated by results of numerical simulations. Tao et al.<sup>[90]</sup> used this sensor to assemble a new system for the field bridge scour monitoring. The performance was quite accurate in the field test. The system included a TDR strip sensor, a TDR signal generator, and a data acquisition system. The TDR strip sensors were partially embedded into the riverbed in the vicinity of bridge abutments or piers (Figure 11a). The sensor was excited by an electromagnetic wave receiving from the control unit. The control unit collected the data and sent them to an Internet workstation. The received data can be analyzed to evaluate bridge scour damage. Many advantages can be displayed when compared to previous TDR sensors. This novel TDR strip sensor can adapt to harsh environments, for example, flood/icing. Also, it can be fabricated to different lengths in order to match the specific requirements. Moreover, it is a composite design with coating at the TDR probes with cost-effective materials.

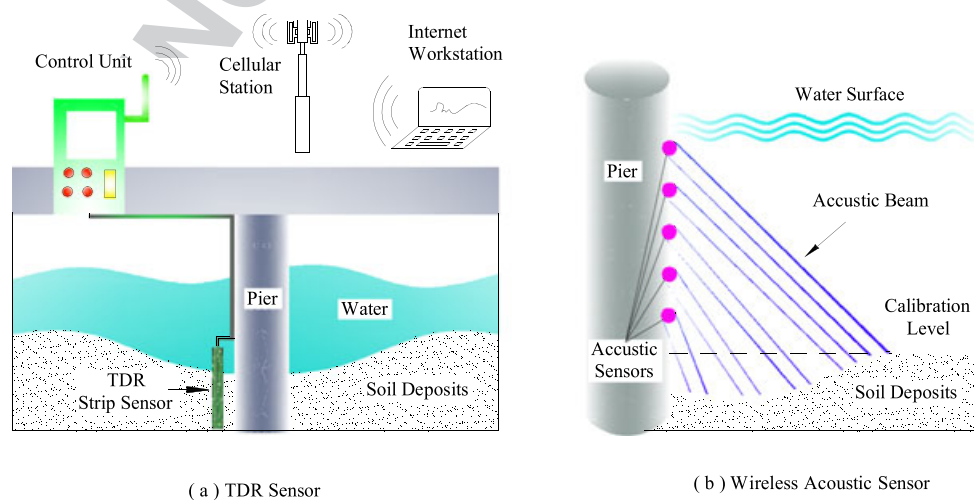


**FIGURE 11** Schematic of (a) TDR sensor and (b) wireless acoustic sensor for scour monitoring [Reproduced from Tao et al. and Dahal et al.<sup>[90,91]</sup>]

Due to these facts, this sensor can be easily installed in the field with durable availability and a low cost during monitoring.

An underwater wireless acoustic sensor has also been proposed for scour depth measurements.<sup>[91]</sup> As shown in Figure 11b, a number of acoustic sensors were tied around to the pier near the water bottom. Sensors in the same bridge pier constituted a cluster and work along their own underwater-gateway. The sensors were oriented to direct acoustic waves to the bottom and receive the reflected waves. Collected signals were sent using acoustic links to the corresponding gateway. Then a surface station could receive the collected signals via the underwater-gateway. Therefore, the scour depth can be measured with the analysis of received signal strength (RSS). Because the transmission loss in water greatly affected the accuracy of the scour depth measurement, a wireless device was used to measure the distance based on RSS short range underwater acoustic communications. The Lambert W function<sup>[92]</sup> that considers the terms of transmission loss was applied to compute distance based on RSS. The performance of this sensor has been validated with numerical simulations. However, more parameters of the environment such as sound scattering and absorption by the sediments should be considered to obtain more accurate results.

Another type of real-time monitoring sensor is the capacitive type sensor.<sup>[93]</sup> The main principle is the change in the capacitance of an electrode pair due to the higher dielectric constant in water than that in soil. The capacitance increases if any soils are scoured and replaced by water. Four or six pairs of electrodes were installed on the river bed around bridge piers. Based on the principle, each pair of electrodes was aligned vertically along piers and considered as a parallel plate capacitor. Due to the different dielectric constants of water and soils, the capacitance would change if soils were washed out between the electrode pairs installed around piers. Bridge scour can be measured by measuring the capacitance of an individual pair of electrodes. However, the change in the capacitance sometimes was so small that it was difficult to precisely detect bridge scour based on this

negligible change in the field test. To address this issue, an AC Wien bridge oscillator circuit is used to measure the change in the capacitance of the electrode. This was because the reciprocal value of this oscillator circuit frequency ( $1/f$ ) was proportional to the square root of the electrode capacitance ( $\sqrt{C_{elect}}$ ). The frequency changes with the value of the electrode capacitance. This frequency can directly reflect the presence of scour. Most importantly, the negligible change in the electrode capacitance can be amplified by measuring the change in the frequency, which is significant for the application of scour detection using the capacitive type sensor. The accuracy of this sensor has been confirmed in the simulations. The primary benefit of this sensor is that it brings little disturbance to the structure and soil, and it can work well in soils and under water. However, its performance in the field is still under ongoing evaluation.

## 7 | DISCUSSIONS

In-depth discussions are made regarding a few controversial and unsolved issues in existing studies. The focus has been placed on the relationship between the PNF and the scour depth in the previous studies. Much less attention has been paid to the effect of the SSI on the accuracy of the measured PNF. Also, there has been rare research on where the valid or the best location(s) of the sensor installation is and on the influence of unsymmetrical shapes of scour holes on the measured PNF. These unsolved issues are discussed in this section, which should be of both theoretical and practical significances to scour detection using the PNF.

The influence of the soil strength on the PNF still remains controversial in previous FEMs. The numerical results from Huang's model<sup>[75]</sup> shown in Figure 12a indicated that the soil strength had a small impact on the measured PNF as different soil strengths led to the negligible differences in the values of the PNF. To investigate different situations, the variation of a Yong's modulus was assumed to linearly increase or decrease from the top to the bottom of the soil layer. However, a different conclusion was obtained in Zhang's model<sup>[76]</sup> presented

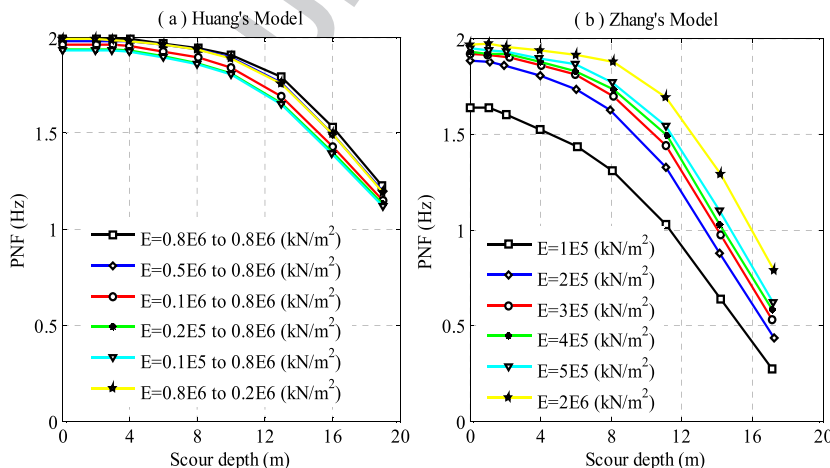


FIGURE 12 Comparison between the numerical results from (a) Huang's and (b) Zhang's model with different soil strengths [Reproduced from Huang et al. and Zhang et al.<sup>[75,76]</sup>]



in Figure 12b where the soil strength obviously influenced the measured PNF. Moreover, the results in this study revealed that the influence of the soil strength was greater at higher values of soil strength (Figure 12b), though the trend of the changes in the PNF was the same as the other soil strengths. The PNF calculated from both the numerical models was at the same order of a magnitude.

Results from another study can help understand this contradiction.<sup>[63]</sup> This study used the pier exposure to simulate different scour situations. The pier exposure increased as scour developed. The PNF was normalized by the PNF obtained from case 3 in Figure 4. The results from Figure 13 indicate that the soil strength has a negligible effect on the PNF when no scour develops. Otherwise, the soil strength explicitly affects the PNF in any scour situations. Because the PNF is very sensitive to the scour damage, the measured PNF should be as precise as possible. Any unacceptable deflections in the measurement of the PNF should be avoided. If the PNF changes by a minor value, for example, about 5%, potential damage should not be ignored because scour-induced bridge failures occur suddenly without any prior warning. This is a particularly critical case during constant torrential rains. Due to the concern, a sensitivity analysis of soil parameters in the soil strength remains contentious. Experimental tests and more accurate numerical models are needed to confirm the conclusions.

Soil types may also deserve further investigations. The noncohesive soils such as highly erodible sands<sup>[54,62]</sup> have been widely utilized in most traditional experiments to find the relationship between the scour depth and the PNF. This type of soil can generate a large scour hole with time economy during the experiment. However, less erodible soils such as cohesive soils may be part of media in the SSI. Therefore, the soils used in the traditional experiments may overestimate scour depths. In fact, the maximum scour

depth with cohesive soils in different flume tests is smaller than that with noncohesive soils.<sup>[94]</sup> Therefore, analyses of the soil types should be conducted to systematically understand the mechanisms of the effect of soil properties on the PNF to advance the framework of the PNF-based scour detection.

Questions regarding the location of the sensor installation also need to be answered. In most previous field and laboratory tests, the dynamic response was usually obtained with sensors at some surface points of bridge components such as the surface of a deck or the top of a pier, or even the bottom of a pier.<sup>[49,61–63]</sup> However, there has been rare research on where the valid or the best location(s) for the sensor installation is. Such research is significant as an inappropriate location may lead to false measurements and an optimal location also ensures better accessibility and signal pick-up. Therefore, the questions would be addressed by measuring the dynamic response of a bridge component at different positions using both experiments and numerical simulations.

Another issue is the influence of the shape of scour holes on the measured PNF, which has also been rarely discussed. Previous numerical and experimental studies simulated scour scenarios by removing equal increments of the surface soil layer or soils evenly around bridge foundations.<sup>[54,62,77]</sup> This type of a scour hole is generally symmetrical. These bridge scour models may fail to reflect the local scour characteristics. In reality, bridge scour may have various different shapes of the scour hole. Among which, many types of the scour holes are unsymmetrical. Limited attention has been paid to the effect of unsymmetrical scour holes on the variation of the measured hole. To address this issue, scour scenarios with the different unsymmetrical scour holes should be developed to investigate their influence on the measured PNF.

It is also worthwhile to mention that the feasibility of PNF-based scour detection has been confirmed by lab-scale tests for simply supported bridges, such as Briaud et al.,<sup>[62]</sup> and by simulations of multispan supported bridges.<sup>[77]</sup> Unfortunately, the performance of this method for other bridge types, such as suspension bridges and arch bridges, has rarely been evaluated and reported in the literature. Theoretically, it is feasible to detect progressive scour for those complicated bridges by investigating the change in the PNF of the entire bridge, for which we can do a simulation to obtain the PNF of the entire bridge using modal analysis. The feasibility of this method has been confirmed using numerical simulations on a real cable-stayed bridge<sup>[78]</sup>; however, it seems difficult to use the PNF of a pier of such a complicated bridge to detect progressive scour in practice. More efforts still need to be made to evaluate the performance of PNF-based scour detection on these complicated types of bridges. In addition, it is very worthwhile to investigate the difference in the PNF vibration feature or trend between scour-caused damage and structure-caused damage. This is because structure-induced damage in reality also can lead to the change in the PNF,

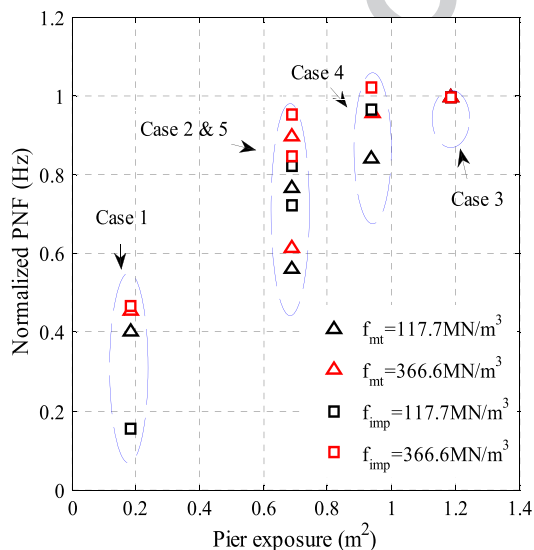


**FIGURE 13** Relationship between different scour situations and the predominant natural frequency in the different soil strength [Reproduced from Samizo et al.<sup>[63]</sup>]

which causes a difficulty in the framework of detecting bridge scour using the PNF if structure-induced damage happens. Therefore, it is always helpful to keep this possibility in mind, and whenever possible, apply the vibration-based method with knowledge from the superstructure inspection, which is relatively easy and common in engineering practice.

## 8 | CONCLUSIONS

Scour detection based on the natural frequency spectrum addresses difficulties in traditional instrument installations and operations, which will possibly provide a more efficient approach for scour monitoring in fields. Many significant findings and innovations have been obtained in the past 5 to 7 years. This paper presents a critical review of the existing studies on the detection and evaluation of bridge scour by estimating the natural frequency spectrum of a bridge or a bridge component. Underlying mechanisms, laboratory and field tests, numerical studies, and vibration data processing schemes were reviewed to summarize the state-of-the-art, which is absent but urgently needed. Updates on recently developed scour monitoring sensors are also provided to complement the introduction.

Future attention is called to highlight the importance of the SSI, for which analyses of the influence of the soil types on the measured predominant natural frequency are particularly limited. Analyses of the effect of the soil strength on the predominant natural frequency from the current evidence also remain contentious. A few unsolved issues, such as the location for the sensor installation and the effect of the shape of scour holes, are also highlighted. Such unsolved issues have been rarely focused in the existing studies but are critical to supplementing and advancing the current framework of scour detection using the natural frequency spectrum.

## REFERENCES

- [1] B. W. Melville, S. E. Coleman, *Bridge Scour*, Water Resources Publication, Highland Ranch, USA **2000**.
- [2] K. Wardhana, F. C. Hadipriono, *J. Perform. Constr. Facil.* **2003**, 17(3), 144.
- [3] A. Shirole, R. Holt. Planning for a comprehensive bridge safety assurance program. *Transportation Research Board 60th Annual Meeting*, Washington, DC, Transportation Research Board, **1991**.
- [4] A. H. E. Elsaid, *Vibration Based Damage Detection of Scour in Coastal Bridges*, [Dissertation], Department of Civil, Construction, and Environmental Engineering, North Carolina State University, Raleigh **2012**.
- [5] G. Chen, B. Schafer, Z. Lin, Y. Huang, O. Suaznabar, J. Shen. Real-time monitoring of bridge scour with magnetic field strength measurement. *Transportation Research Board 92nd Annual Meeting*, Washington, DC, Transportation Research Board, **2013**.
- [6] P. F. Lagasse, L. Zevenbergen, W. Spitz, L. Arneson. Stream stability at highway structures. FHWA-HIF-12-004, Transportation Research Board, Washington, DC **2012**.
- [7] P. F. Lagasse. Instrumentation for measuring scour at bridge piers and abutments. *Transportation Research Board 76th Annual Meeting*, Washington, DC, Transportation Research Board, **1997**.
- [8] Xinhua-Net. Images memory of floods and droughts. **2010**. [http://www.yn.xinhuanet.com/newscenter/2010-12/15/content\\_21632481\\_3.htm](http://www.yn.xinhuanet.com/newscenter/2010-12/15/content_21632481_3.htm) (Accessed: 2 Feb. 2014).
- [9] Xinhua-Channel. A report of the bridge collapse caused by the flood. **2013**. <http://roll.sohu.com/20130710/n381187682.shtml> (Accessed: 2 Feb. 2014).
- [10] L. Hamill, *Bridge Hydraulics*, CRC Press, New York, USA **1999**.
- [11] R. Ettema, B. Yoon, T. Nakato, M. Muste, *KSCE J. Civ. Eng.* **2004**, 8(6), 643.
- [12] S.-Y. Lim, *J. Hydraul. Eng.* **1997**, 123(3), 237.
- [13] B. Melville, A. Sutherland, *J. Hydraul. Eng.* **1988**, 114(10), 1210.
- [14] S. C. Jain, E. E. Fischer. Scour around circular bridge piers at high Froude numbers. FHWA-RD-79-104 Final Rpt., Federal Highway Administration, University of Iowa, Iowa City, USA **1979**.
- [15] S.-U. Choi, S. Cheong, *J. Am. Water Resour. Assoc.* **2006**, 42(2), 487.
- [16] M. Najafzadeh, H. M. Azamathulla, *J. Comput. Civ. Eng.* **2013**, 1. Q3
- [17] S. M. Bateni, S. Borghei, D.-S. Jeng, *Eng. Appl. Artif. Intel.* **2007**, 20(3), 401.
- [18] M. Zounemat-Kermani, A.-A. Beheshti, B. Ataie-Ashtiani, S.-R. Sabbagh-Yazdi, *Appl. Soft Comput.* **2009**, 9(2), 746.
- [19] J. E. Richardson, V. G. Panchang, *J. Hydraul. Eng.* **1998**, 124(5), 530.
- [20] Z. Zhao, H. Fernando, *Environ. Fluid Mech.* **2007**, 7(2), 121.
- [21] Y. Jia, T. Kitamura, S. S. Wang, *J. Hydraul. Eng.* **2001**, 127(3), 219.
- [22] H. Zhu, X. Qi, P. Lin, Y. Yang, *Appl. Ocean Res.* **2013**, 41, 87.
- [23] M. Dixen, B. M. Sumer, J. Fredsøe, *Coast. Eng.* **2013**, 73, 84.
- [24] A. Khosronejad, C. Hill, S. Kang, F. Sotiropoulos, *Adv. Water Resour.* **2013**, 54, 191.
- [25] X. Zhao, W. Li, G. Song, Z. Zhu, J. Du, *Sensors* **2013**, 13(2), 1490.
- [26] Z. G. Bai, R. C. Lv, R. Meng, *Appl. Mech. Mater.* **2013**, 256, 1956.
- [27] Y. M. Hong, M. L. Chang, H. C. Lin, Y. C. Kan, C. C. Lin, *Appl. Mech. Mater.* **2012**, 121, 162.
- [28] F. Z. Li, A. Dwivedi, Y. M. Low, J.-H. Hong, Y.-M. Chiew, *J. Eng. Mech.* **2012**, 139(7), 868.
- [29] J.-L. Briaud, S. Hurlbaeus, K.-A. Chang, C. Yao, H. Sharma, O.-Y. Yu, C. Darby, B. E. Hunt, G. R. Price. Realtime monitoring of bridge scour using remote monitoring technology. No. FHWA/TX-11/0-6060-1, Texas Transportation Institute, Texas A&M University System **2011**.
- [30] A. Roulund, B. M. Sumer, J. Fredsøe, J. Michelsen, *J. Fluid Mech.* **2005**, 534, 351.
- [31] B. Mutlu Sumer, *J. Hydraul. Res.* **2007**, 45(6), 723.
- [32] A. Tafarajnoruz, R. Gaudio, S. Dey, *J. Hydraul. Res.* **2010**, 48(4), 441.
- [33] S. Millard, J. Bungey, C. Thomas, M. Soutsos, M. Shaw, A. Patterson, *NDT & E Int.* **1998**, 31(4), 251.
- [34] P. Inchan, L. Joengwoo, C. Woncheol. Assessment of bridge scour and riverbed variation by a ground penetrating radar. *Proceedings of the Tenth International Conference on Ground Penetrating Radar*, Delft, The Netherlands, IEEE, **2004**.
- [35] M. Forde, D. McCann, M. Clark, K. Broughton, P. Fenning, A. Brown, *Ndt & E Int.* **1999**, 32(8), 481.
- [36] L. Prendergast, K. Gavin, *J. Rock Mech. Geotech. Eng.* **2014**, 6(2), 138.
- [37] S. Villalba, J. R. Casas, *Mech. Syst. Signal Process.* **2013**, 39(1), 441.
- [38] H. Sohn, C. R. Farrar, F. M. Hemez, D. D. Shunk, D. W. Stinemat, B. R. Nadler, J. J. Czarniecki. A review of structural health monitoring literature: 1996-2001: Los Alamos National Laboratory Los Alamos, NM, **2004**.
- [39] A. Zarafshan, A. Iranmanesh, F. Ansari, *J. Bridge Eng.* **2011**, 17(6), 829.
- [40] L. Deng, C. Cai, *Pract. Period. Struct. Des. Construct.* **2009**, 15(2), 125.
- [41] N. L. Anderson, A. M. Ismael, T. Thitimakorn, *Environ. Eng. Geosci.* **2007**, 13(1), 1.
- [42] H. Nassif, A. O. Ertekin, J. Davis. Evaluation of bridge scour monitoring methods, United States Department of Transportation, Federal Highway Administration, Trenton, **2002**.

- [43] H. Wang, C.-Y. Wang, C. Lin, H.-C. Liu, C.-H. Hu, M.-H. Chen. A forensic study on the collapse of Shuang-Yuan Bridge during Typhoon Morakot in Taiwan. *Proceedings of the 5th Civil Engineering Conference in the Asian Region (CECAR5) and Australasian Structural Engineering Conference* Sydney, Australia, **2010**.
- [44] Y.-B. Lin, K.-C. Chang, C.-C. Chen, S.-C. Wong, L.-S. Lee, Y.-K. Wang, M.-H. Gu, *Int. J. Autom. Smart Technol.* **2011**, 1(2), 51.
- [45] J.-Y. Lu, J.-H. Hong, C.-C. Su, C.-Y. Wang, J.-S. Lai, *J. Hydraul. Eng.* **2008**, 134(6), 810.
- [46] C.-Y. Wang, H.-L. Wang, C.-C. Ho, *Adv. Struct. Eng.* **2012**, 15(6), 897.
- [47] O. Salawu, *Eng. Struct.* **1997**, 19(9), 718.
- [48] J. Humar, *Dynamics of Structures*, CRC Press, London, U.K. **2012**.
- [49] Y. Ko, W. Lee, W. Chang, H. Mei, C. Chen. Scour evaluation of bridge foundations using vibration measurement. *5th International Conference on Scour and Erosion*, San Francisco, CA, USA, **2010**.
- [50] O. S. Salawu, C. Williams, *Eng. Struct.* **1995**, 17(2), 113.
- [51] M. Biswas, A. Pandey, M. Samman, *Int. J. Anal. Exp. Modal Anal.* **1990**, 5(1), 33.
- [52] M. Shinoda, H. Haya, S. Murata. Nondestructive evaluation of railway bridge substructures by percussion test. *Fourth International Conference on Scour and Erosion*, Tokyo, Japan, The Japanese Geotechnical Society, **2008**.
- [53] C. Yao, C. Darby, O.-Y. Yu, S. Hurlbeaus, K.-A. Chang, J. Price, B. Hunt, J.-L. Briaud. Motion sensors for scour monitoring: laboratory experiment with a shallow foundation. *GeoFlorida 2010: Advances in Analysis, Modeling & Design*, West Palm Beach, USA, GeoFlorida, **2010**.
- [54] L. Prendergast, D. Hester, K. Gavin, J. O'Sullivan, *J. Sound Vib.* **2013**, 332(25), 6685.
- [55] C. Lin, Y. Yang, *Eng. Struct.* **2005**, 27(13), 1865.
- [56] Y.-B. Yang, C. Lin, J. Yau, *J. Sound Vib.* **2004**, 272(3), 471.
- [57] Y. Yang, K. Chang, *Eng. Struct.* **2009**, 31(10), 2448.
- [58] Y. Yang, K. Chang, Y. Li, *Eng. Struct.* **2013**, 48, 353.
- [59] Y. Yang, K. Chang, *J. Sound Vib.* **2009**, 322(4), 718.
- [60] Y. Masui, O. Suzuki, *JR East Tech. Rev.* **2009**, 14(14), 65.
- [61] C. Yao, C. Darby, S. Hurlbeaus, G. Price, H. Sharma, B. Hunt, O. Yu, K. Chang, J. Briaud. Scour monitoring development for two bridges in Texas. *5th International Conference on Scour and Erosion*, San Francisco, CA, USA, Scour and Erosion, **2010**.
- [62] J. L. Briaud, C. Yao, C. Darby, H. Sharma, S. Hurlbeaus, G. Price, K. Chang, B. Hunt, O. Y. Yu. Motion sensors for scour monitoring: laboratory experiments and numerical simulations. *Transportation Research Board (TRB) 89th Annual Meeting*, Washington, DC, Transportation Research Board **2010**.
- [63] M. Samizo, S. Watanabe, T. Sugiyama, K. Okada. Evaluation of the structural integrity of bridge pier foundations using microtremors in flood conditions. *International Conference on Scour and Erosion 2010*, San Francisco, CA, USA, Scour and Erosion, **2010**.
- [64] T.-H. Lin, Y.-C. Lu, S.-L. Hung. Field Study of Bridge Scour Using Imote2. NET-Based Wireless Monitoring System. *The 6th International Workshop on Advanced Smart Materials and Smart Structures Technology*, **2011**.
- [65] S. Foti, D. Sabia, *J. Bridge Eng.* **2011**, 16(2), 295.
- [66] T. K. Lin, Y. P. Wang, M. C. Huang, C. A. Tsai. Implementation of a vibration-based bridge health monitoring system on scour issue. *Applied Mechanics and Materials*, Trans Tech Publ, **2013**.
- [67] H.-P. Tserng, S.-H. Ju, C.-W. Feng, Y.-J. Chang, Y.-R. Lin, *Int. J. Eng. Technol.* **2013**, 5(5), 641.
- [68] M. Novak, *Can. Geotech. J.* **1974**, 11(4), 574.
- [69] S. C. Dutta, R. Roy, *Comput. Struct.* **2002**, 80(20), 1579.
- [70] C. W. Feng, S. H. Ju, H. Y. Huang, P. S. Chang. Using genetic algorithms to estimate the scour depth around the bridge pier. *Proc. 28th International Symposium on Automation and Robotics in Construction*, Seoul, Korea, ISARCs, **2011**.
- [71] F. Naeim, *Earthq. Spectra* **2007**, 23(2), 491.
- [72] C. W. Feng, H. Y. Huang, S. H. Ju, *Int. J. Eng. Technol.* **2013**, 5(4), 462.
- [73] D. E. Goldberg, *Genetic Algorithms*, India, Pearson Education **2006**.
- [74] S. S. Halli, K. V. Rao, *Advanced Techniques of Population Analysis*, Springer, New York, USA **1992**.
- [75] H. Y. Huang, W. Y. Chou, S. H. Ju, C. W. Feng. Application of finite element method and genetic algorithms in bridge scour detection. *Society for Social Management Systems Internet Journal*. **2012**. <http://hdl.handle.net/10173/1027>.
- [76] X. Zhang, Y. Chen, W. Yao, *J. Appl. Sci.* **2013**, 6(1), 102.
- [77] S. Ju, *Soil Dynam. Earthquake Eng.* **2013**, 55, 247.
- [78] C.-C. Chen, W.-H. Wu, F. Shih, S.-W. Wang, *NDT & E Int.* **2014**, 66, 16.
- [79] M. Fahey, *Can. Geotech. J.* **1992**, 29(1), 157.
- [80] J.-B. Bodeux, J.-C. Golinval, *Smart Mater. Struct.* **2001**, 10(3), 479.
- [81] N. M. M. Maia, J. M. M. e Silva, *Theoretical and Experimental Modal Analysis*, Research Studies Press, Taunton, U.K. **1997**.
- [82] L. Lennart, *System Identification: Theory for the User*, Prentice Hall PTR, New Jersey, USA **1999**.
- [83] J. N. Juang, *Applied System Identification*, Prentice Hall, New York, USA **1994**.
- [84] A. H. Elsaid, R. Seracino. Vibration based damage detections of scour in coastal bridges. *Homeland Security Affairs*. **2012**. <http://hdl.handle.net/10945/25008>.
- [85] M. Abdel Wahab, G. De Roeck, *J. Sound Vib.* **1999**, 226(2), 217.
- [86] B. Wu, W. Chen, H. Li. Real-time monitoring of bridge scouring using ultrasonic sensing technology. *SPIE Smart Structures and Materials & Nondestructive Evaluation and Health Monitoring*, San Diego, CA, USA, **2012**.
- [87] D. P. Genda Chen, Z. Zhou, Y. Huang, A. Radchenko, Inventor. Sensors for integrated monitoring and mitigation erosion, **2013**.
- [88] A. Radchenko, D. Pommerenke, G. Chen, P. Maheshwari, S. Shinde, V. Pilla, Y. R. Zheng. Real time bridge scour monitoring with magneto-inductive field coupling. *SPIE Smart Structures and Materials; Nondestructive Evaluation and Health Monitoring*, San Diego, CA, USA, International Society for Optics and Photonics, **2013**.
- [89] X. Yu, B. Zhang, J. Tao, X. Yu, *Struct. Health Monit.* **2013**, 12(2), 99.
- [90] J. Tao, X. Yu, X. Yu. Real-time TDR field bridge scour monitoring system. *Structures Congress*, Pittsburgh, USA, ASCE, **2013**.
- [91] P. Dahal, D. Peng, Y. L. Yang, H. Sharif, *Comm. Netw.* **2013**, 5(3), 641.
- [92] M. Hosseini, H. Chizari, C. K. Soon, R. Budiarto. RSS-based distance measurement in Underwater Acoustic Sensor Networks: an application of the Lambert W function. *2010 4th International Conference on Signal Processing and Communication Systems (ICSPCS)*, IEEE, **2010**.
- [93] S. Motakabber, M. I. Ibrahimy, A. Alam. Real-time bridge scour monitoring system by using capacitor sensor. *Third International Conference on Geotechnique*, Nagoya, Japan, **2013**.
- [94] S. J. Oh, J.-L. Briaud, K.-A. Chang, H.-C. Chen. Maximum Abutment Scour Depth in Cohesive Soils. *International Conference on Scour and Erosion 2010*, San Francisco, CA, USA, Scour and Erosion, **2010**.

**How to cite this article:** Bao, T., and Liu, Z. (2016), Vibration-based bridge scour detection: A review, *Struct. Control Health Monit.*, doi: 10.1002/stc.1937

# Author Query Form

---

**Journal: Structural Control and Health Monitoring**

**Article: stc\_1937**

Dear Author,

During the copyediting of your paper, the following queries arose. Please respond to these by annotating your proofs with the necessary changes/additions.

- If you intend to annotate your proof electronically, please refer to the E-annotation guidelines.
- If you intend to annotate your proof by means of hard-copy mark-up, please use the standard proofing marks. If manually writing corrections on your proof and returning it by fax, do not write too close to the edge of the paper. Please remember that illegible mark-ups may delay publication.

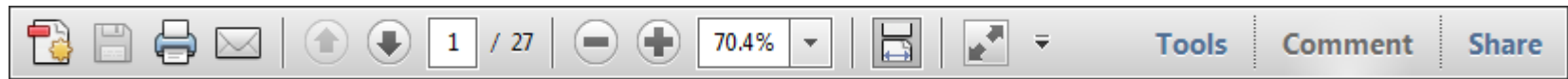
Whether you opt for hard-copy or electronic annotation of your proofs, we recommend that you provide additional clarification of answers to queries by entering your answers on the query sheet, in addition to the text mark-up.

Query No.	Query	Remark
Q1	AUTHOR: Please confirm that given names (red) and surnames/family names (green) have been identified correctly.	
Q2	AUTHOR: Please check if "Yong's modulus" should be changed to "Young's modulus."	
Q3	AUTHOR: Please provide the volume number for reference 16.	

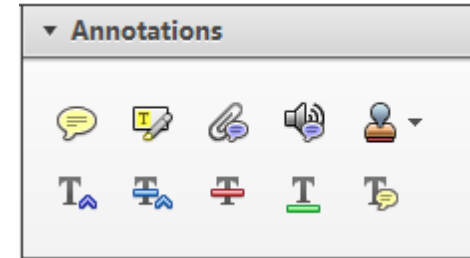
Required software to e-annotate PDFs: **Adobe Acrobat Professional** or **Adobe Reader** (version 7.0 or above). (Note that this document uses screenshots from **Adobe Reader X**)

The latest version of Acrobat Reader can be downloaded for free at: <http://get.adobe.com/uk/reader/>

Once you have Acrobat Reader open on your computer, click on the **Comment** tab at the right of the toolbar:



This will open up a panel down the right side of the document. The majority of tools you will use for annotating your proof will be in the **Annotations** section, pictured opposite. We've picked out some of these tools below:



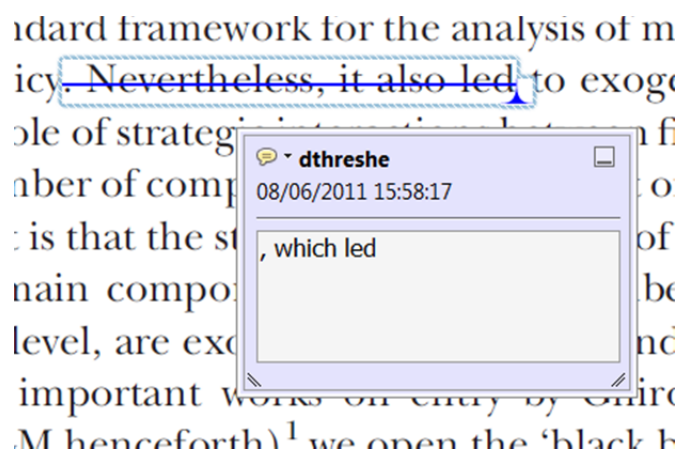
**1. Replace (Ins) Tool – for replacing text.**



Strikes a line through text and opens up a text box where replacement text can be entered.

**How to use it**

- Highlight a word or sentence.
- Click on the **Replace (Ins)** icon in the Annotations section.
- Type the replacement text into the blue box that appears.



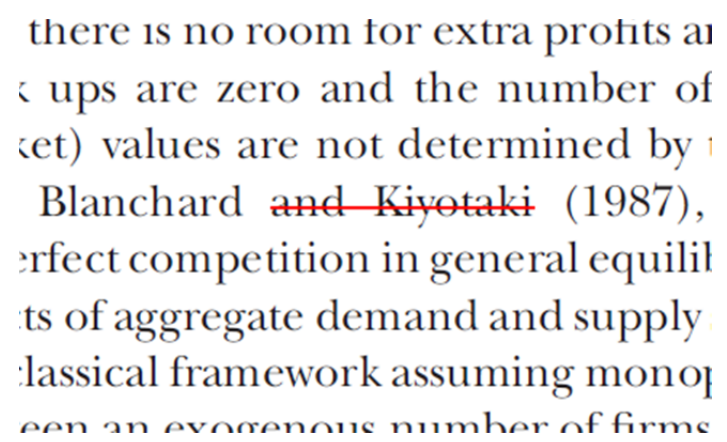
**2. Strikethrough (Del) Tool – for deleting text.**



Strikes a red line through text that is to be deleted.

**How to use it**

- Highlight a word or sentence.
- Click on the **Strikethrough (Del)** icon in the Annotations section.



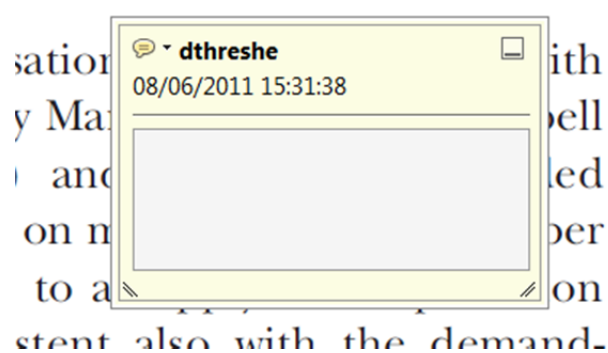
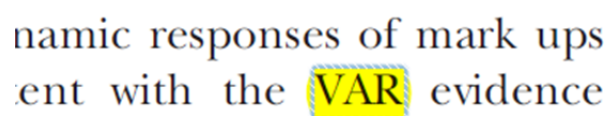
**3. Add note to text Tool – for highlighting a section to be changed to bold or italic.**



Highlights text in yellow and opens up a text box where comments can be entered.

**How to use it**

- Highlight the relevant section of text.
- Click on the **Add note to text** icon in the Annotations section.
- Type instruction on what should be changed regarding the text into the yellow box that appears.



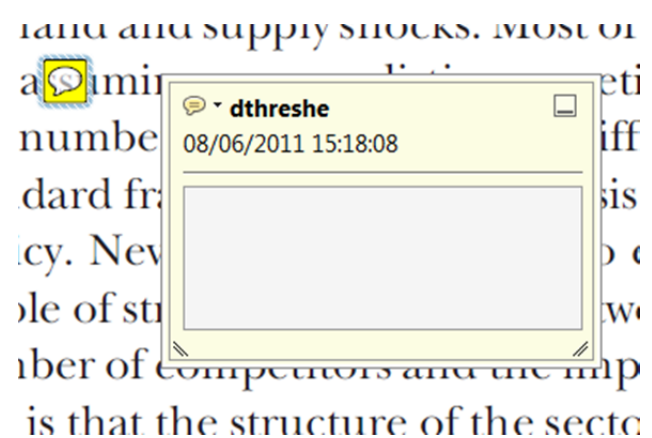
**4. Add sticky note Tool – for making notes at specific points in the text.**



Marks a point in the proof where a comment needs to be highlighted.

**How to use it**

- Click on the **Add sticky note** icon in the Annotations section.
- Click at the point in the proof where the comment should be inserted.
- Type the comment into the yellow box that appears.



USING e-ANNOTATION TOOLS FOR ELECTRONIC PROOF CORRECTION

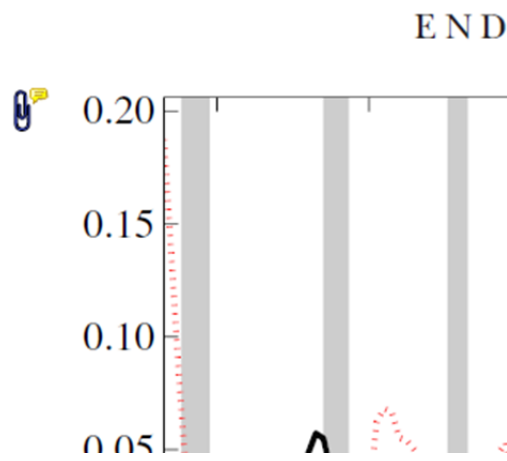
**5. Attach File Tool – for inserting large amounts of text or replacement figures.**



Inserts an icon linking to the attached file in the appropriate place in the text.

**How to use it**

- Click on the [Attach File](#) icon in the Annotations section.
- Click on the proof to where you'd like the attached file to be linked.
- Select the file to be attached from your computer or network.
- Select the colour and type of icon that will appear in the proof. Click OK.



**6. Add stamp Tool – for approving a proof if no corrections are required.**

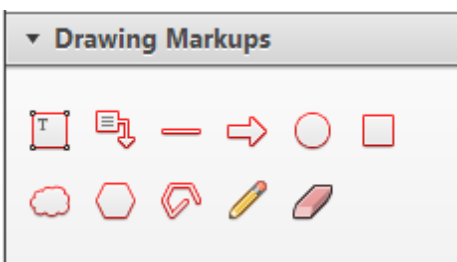


Inserts a selected stamp onto an appropriate place in the proof.

**How to use it**

- Click on the [Add stamp](#) icon in the Annotations section.
- Select the stamp you want to use. (The [Approved](#) stamp is usually available directly in the menu that appears).
- Click on the proof where you'd like the stamp to appear. (Where a proof is to be approved as it is, this would normally be on the first page).

of the business cycle, starting with the  
 on perfect competition, constant return  
 production. In this environment goods  
 extra profits and the number of firms  
 he number of firms is determined by the model. The New-Key  
 otaki (1987), has introduced product  
 general equilibrium models with nomin  
 ed and supply shocks. Most of this literat

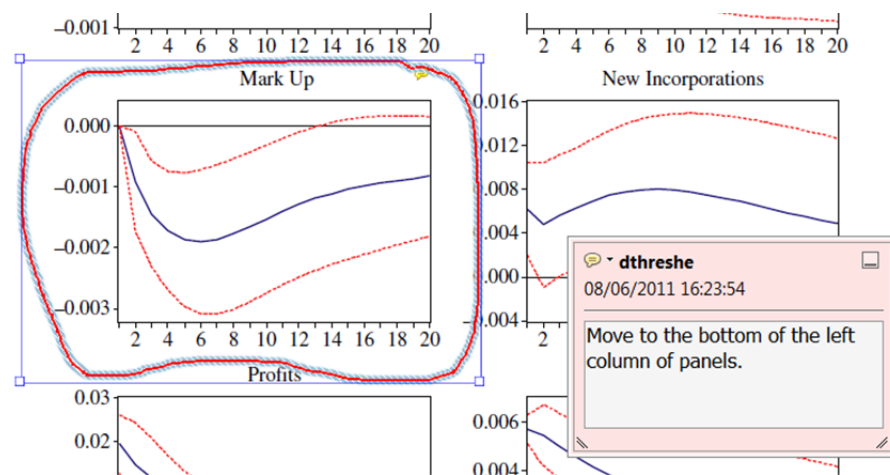


**7. Drawing Markups Tools – for drawing shapes, lines and freeform annotations on proofs and commenting on these marks.**

Allows shapes, lines and freeform annotations to be drawn on proofs and for comment to be made on these marks..

**How to use it**

- Click on one of the shapes in the [Drawing Markups](#) section.
- Click on the proof at the relevant point and draw the selected shape with the cursor.
- To add a comment to the drawn shape, move the cursor over the shape until an arrowhead appears.
- Double click on the shape and type any text in the red box that appears.



For further information on how to annotate proofs, click on the [Help](#) menu to reveal a list of further options:

